International Journal of Earth Sciences (2019) 108:1333–1350
https://doi.org/10.1007/s00531-019-01709-7

ORIGINAL PAPER

# Field documentation and genesis of back-structures in ductile and brittle regimes from the foreland part of a collisional orogen: examples from the Darjeeling–Sikkim Lesser Himalaya, India

**Narayan Bose**[1] · **Soumyajit Mukherjee**[1]

Received: 9 February 2019 / Accepted: 27 March 2019 / Published online: 9 April 2019


**Abstract**

In the foreland-side of an orogen, thrust-related structures develop that verge towards the foreland (fore-thrusts). Although much less abundant, structures with opposite vergence (i.e., towards hinterland), named, back-structures, also exist. We report back-structures (exposure scale back-thrusts and associated folds) from the Darjeeling Sikkim Lesser Himalaya, India. These structures occur mainly in three Back-Structure Zones (BSZ-A, -B, and C). Back-structures probably originated in the ductile regime and continued in the brittle domain. Tectonic setting of the study area, such as- critical taper, duplexing, etc. indicates a good potential for the presence of back-structures in this region. Along with the previous work on back-structures in collisional orogens, Himalaya in particular, these structures seem to be ubiquitous. The correlation of field observations with tectonics indicate that mechanisms, e.g., critical taper, sub-surface barriers, and passive roof duplex played roles in forming back-structures in this part of the Sikkim Lesser Himalaya.

**Keywords** Collisional orogen · Tectonics · Deformation mechanism · Meso-scale deformation · Brittle shear zone · Regional faults

## Introduction

The Himalayan mountain chain is formed by continent–continent collision between the Indian and the Eurasian plates, ~ 54 Ma back (recent reviews in Hu et al. 2016; Najman et al. 2017; Webb et al. 2017). Collisional orogens are characterized by compressional fore-thrusts that dip towards the hinterland and verge towards the foreland-side. Such thrusts accommodate significant crustal shortening (e.g., Yin 2006 and references there in; Mukherjee 2013a; Bhattacharyya and Ahmed 2016). But, although less numerous, thrusts with opposite dip direction, i.e., towards foreland and with opposite vergence towards the hinterland, also exist and are termed as back-thrusts (Fig. 1). Previous workers have documented back-thrusts from several collisional orogens, e.g., Zagros (Molinaro et al. 2004), Alps (Platt et al. 1989), western Pyrenees (Dumont et al. 2015), and the Himalaya (Mukherjee 2013b; Dutta et al. 2019; Mahato et al. 2019). Study of back-structures is of great importance in collisional orogens since (i) those might be related to seismicity (e.g., Buttinelli et al. 2016; Zhang et al. 2016; Jayangondaperumal et al. 2017); (ii) they seem to constitute integral parts of collisional orogens (e.g., Sun et al. 2016; Zelilidis et al. 2016); and (iii) structural traps for hydrocarbon might consist of those structures (Butler et al. 2004; Hao et al. 2016). Back-thrusts have been deciphered mainly from geological field studies (Carmignani et al. 1994; Thakur et al. 2007; Samimi and Gholami 2017), cross-section balancing (Erslev 1993) and seismic studies (Namson and Davis 1988; Li et al. 2016; Shah and Abdullah 2017). Analogue- and analytical-models too simulate back-thrusts and back-folds (e.g., Rodgers and Rizer 1981; Dotare et al. 2016; Li and Mitra 2017).

Back-structures have already been documented in the Himalaya, from the Siwalik range of Nepal (e.g., Mugnier et al. 1998), and that of India (Dutta et al. 2019), Lesser Himalaya in Himachal Pradesh state (India) (Mukhopadhyay

**Electronic supplementary material** The online version of this article (https://doi.org/10.1007/s00531-019-01709-7) contains supplementary material, which is available to authorized users.

✉ Soumyajit Mukherjee
soumyajitm@gmail.com

[1] Department of Earth Sciences, Indian Institute of Technology Bombay, Powai, Mumbai, Maharashtra 400 076, India

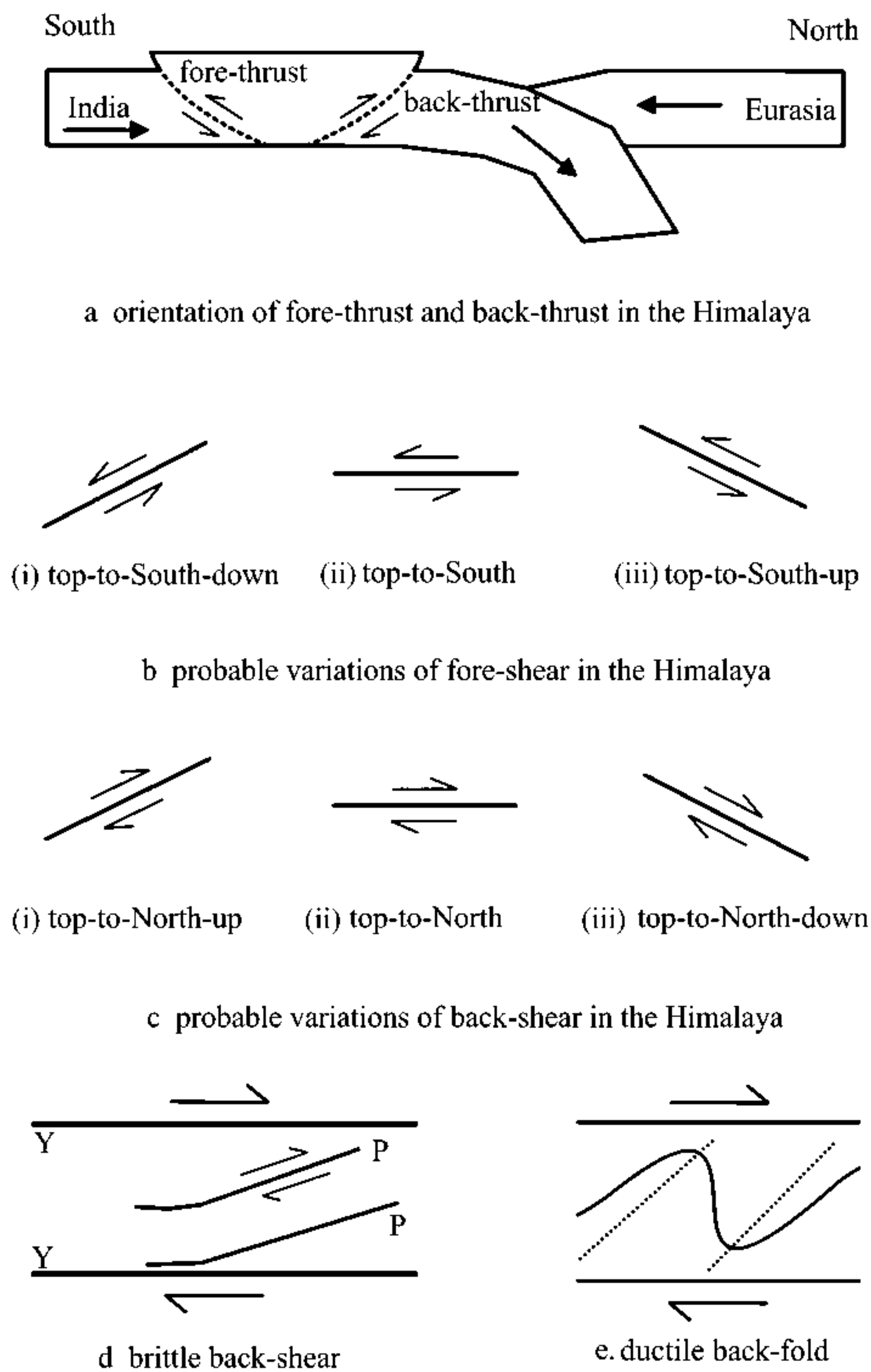


**Fig. 1** Schematic diagrams: **a** orientations of fore- and back-shears in the Himalaya. **b**, **c** Shear senses related to fore- and back- shears, respectively. **d**, **e** Vergence of brittle back-shear and ductile back-fold, respectively. In this study, both of them have been clubbed under the term "back-structure"

and Mishra 2005), and the Greater Himalayan Crystallines (or the Higher Himalaya) at the Bhagirathi river sections, Uttarakhand state (India) (Mukherjee 2013b). Back-folds present in the hanging wall of the South Tibetan Detachment (STD) of the Nepalese Himalaya, originated prior to the extensional (normal) slip of the STD (Fig. 2 of Godin et al. 1999). Hence, although these back-folds occur on the hanging wall of a normal fault, i.e., the STD, they were formed by Himalayan compression. From the Siwalik range of Himachal Pradesh (NW India), Jayangondaperumal et al. (2017) report coeval fore- and back-thrusting, but the movement along back-thrust is episodic. Based on AFT dating, Patel et al. (2015) and Singh and Patel (2017) report back-thrusting of the North Almora Thrust (Kumaun Uttarakhand Himalaya) younger than the corresponding fore-thrusts. In the Kumaun Lesser Himalaya, the North Almora Thrust and the nearby Kasun Thrust reactivated as back-thrust during rapid exhumation (0.58 mma$^{-1}$) at ~ 14 Ma (Patel et al. 2015; Agarwal et al. 2016; Singh and Patel 2017).

In this context, this study has been conducted to document the exposure-scale back-thrusts and to understand their genesis. Here we use the term "back-structures" to describe collectively such exposure-scale back-thrusts in ductile and brittle regimes and associated folds. In meso-scale, the shear sense of such back-structures can be observed in terms of the angular relationship between the brittle Y- and the P-planes, and between the C- and the S-planes in ductile regime (e.g., Mukherjee 2013a), deformed quartz veins, etc. In the ductile domain, hinterland verging back-folds can also develop (Dumont et al. 2015). For example, Avé Lallemant and Oldow's (1998) report back folds from the Brooks Range, Alaska. The prerequisites of back-thrust formation (review in Xu et al. 2015) are brittle rheology, presence of ramp/fault bend, strain build-up zones, etc. These criteria match well with the configuration of the Lesser Himalaya, which is made up of Proterozoic (meta-) sediments (review by Yin 2006) and being deformed in brittle critical taper mechanism. Here the ongoing Himalayan tectonic compression results in high strain build-up, which is reflected through intense duplexing (Srivastava and Mitra 1994; He et al. 2015; Carosi et al. 2016) and frequent seismicity. Hence, the Lesser Himalaya is a favorable place to host back-structures, and the Darjeeling–Sikkim Himalaya (DSH) has been chosen in this study.

## Geological setting

As its geographic name suggests, the DSH is distributed over the Darjeeling district (West Bengal state) and Sikkim state of India, i.e., between the longitudes 88°50′E and 88°47′E. It is surrounded by the Nepal Himalaya in the west, the Bhutan Himalaya in the east, the Tibetan Plateau in the north and the Bengal Basin in the south. Most of the pioneering works, including the geological mapping of this region, were done by the Geological Survey of India (e.g., references in Basu 2013).

### Framework

Towards north, the major tectonic discontinuities in the DSH (Fig. 2) are the Main Frontal Thrust (MFT), the Main Boundary Thrust (MBT = South Kalijhora Thrust: Mukul 2000), the Ramgarh Thrust (RT = North Kalijhora thrust: Mukul 2000 = Daling Thrust: e.g., Bose et al. 2014), the Main Central Thrust(s) (MCT/MCTZ/MCT$_1$, MCT$_2$, etc.) and the Sothern Tibetan Detachment (STD). Based on mapping, structural and geochronological analyses, Carosi et al. (2018) plot a Higher Himalayan Discontinuity to be present between MCT and STD. From field observations, many workers have demarcated the STD as a back-thrust (e.g., Webb et al. 2011; Webb and He 2012). The DSH is a zone of active tectonics with a minimum ~ 12 mm y$^{-1}$ rate of convergence at present (Mukul 2010). Demarcated by the Main Boundary Thrust (MBT) at S and the Main Central Thrust Zone (MCTZ) at N, the Lesser Himalayan (LH) in Sikkim is exposed as the Teesta half-window (Neogi et al. 1998).

### Lithology

The Teesta half-window consists of Daling-, Buxa- and Gondwana rocks, and the intrusives of Lingste Gneiss. The LH mainly consists of Palaeoproterozoic metapelites viz., slates, phyllites, (psammo-pelitic) schists, greywackes, etc. (Gangopadhyay and Ray 1978). In this half-window, the Daling Group separates from the underlying Gondwana units and the Buxa Formation by the Ramgarh Thrust (RT, = North Kalijhora Thrust: Mukul 2000). RT co-activated with the MCTZ possibly ~ 10 Ma back (Mukul 2010) defining a roof thrust for the Lesser Himalayan duplex (Bhattacharyya and Mitra 2009; Robinson and Pearson 2013). The Lesser Himalayan duplex zone shows the highest exhumation rate: 2.6–3.5 mm y$^{-1}$, as per the numerical modeling by Landry et al. (2016). The simplified litho-tectonic setting of the Lesser Himalaya in DSH is (after Parui and Bhattacharyya 2018 and references therein):

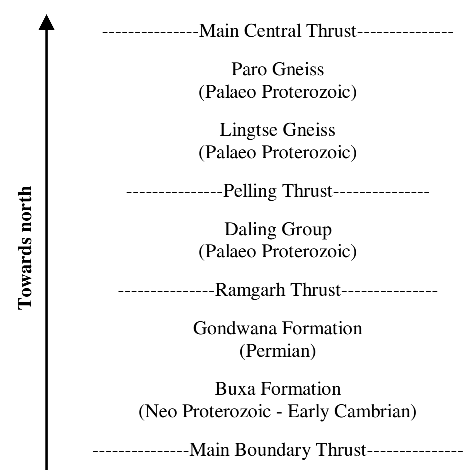


### Deformation history

Three stages of folding have been reported commonly from the Lesser Himalaya in Sikkim (Supplementary Table 1). The characteristic features of those phases are: D$_1$- related to F$_1$ folding and S$_1$ axial-plane foliation, D$_2$- related to F$_2$ folding and S$_2$ crenulations, and D$_3$- related to F$_3$ folding and S3 axial-plane crenulations. The axial plane schistosity

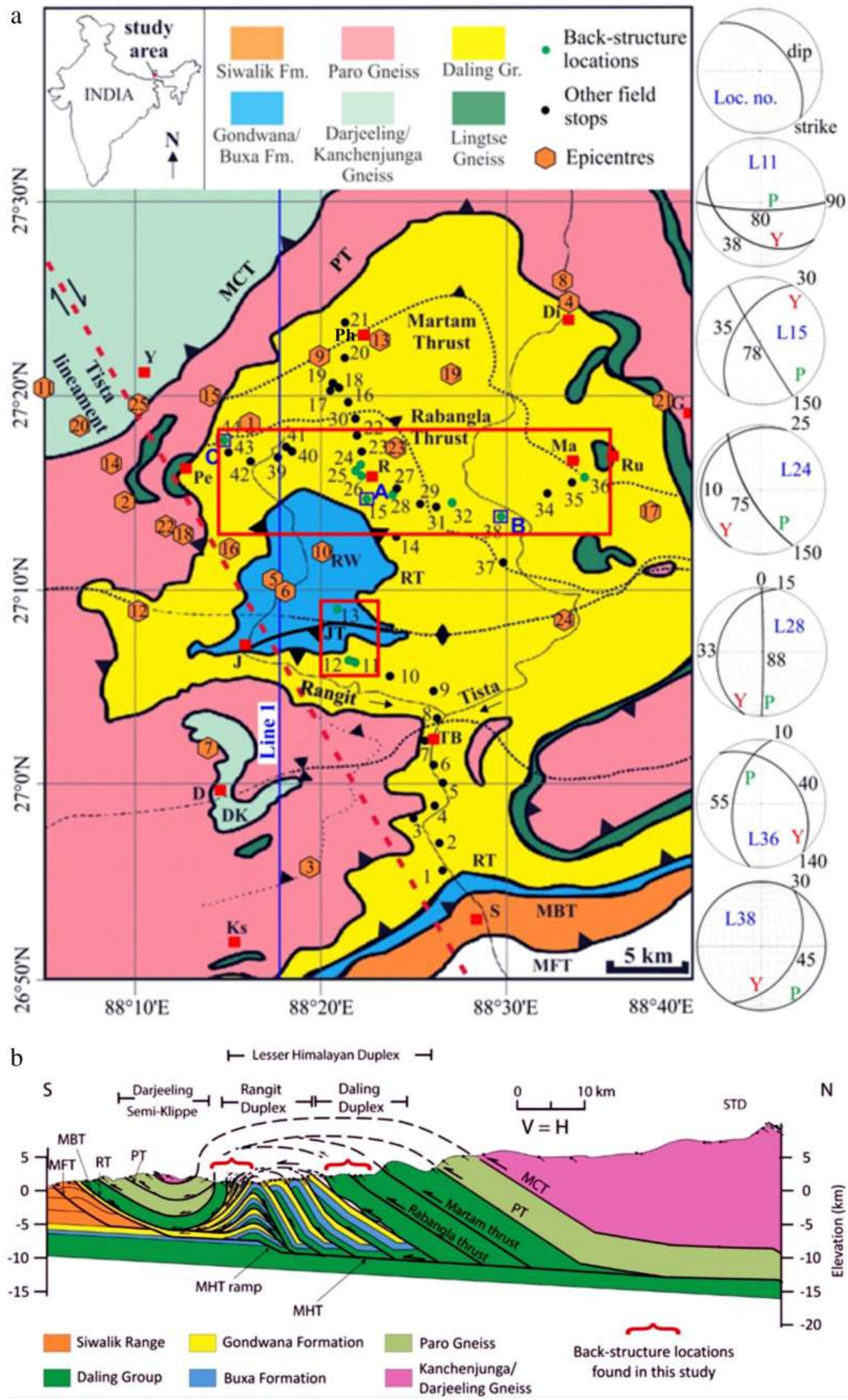
a
study area
INDIA
N
Siwalik Fm.
Paro Gneiss
Daling Gr.
Back-structure locations
Other field stops
Epicentres
Gondwana/ Buxa Fm.
Darjeeling/ Kanchenjunga Gneiss
Lingtse Gneiss
dip
Loc. no.
strike
L11
L15
L24
L28
L36
L38
27°30'N
27°20'N
27°10'N
27°0'N
26°50'N
88°10'E
88°20'E
88°30'E
88°40'E
MCT
PT
Tista lineament
Martam Thrust
Rabangla Thrust
RW
RT
JT
Rangit
Tista
Line 1
MBT
MFT
5 km
b
Lesser Himalayan Duplex
S
N
Darjeeling Semi-Klippe
Rangit Duplex
Daling Duplex
0 10 km
V = H
STD
MBT
MFT
RT
PT
MCT
Martam thrust
Rabangla thrust
MHT ramp
MHT
Elevation (km)
Siwalik Range
Gondwana Formation
Paro Gneiss
Back-structure locations found in this study
Daling Group
Buxa Formation
Kanchenjunga/ Darjeeling Gneiss

◂**Fig. 2** **a** Field locations plotted on a geological map of the Darjeeling–Sikkim Himalaya (redrawn after Fig. 2 of Bhattacharyya and Mitra 2009 and Fig. 1 of Das et al. 2016). Mapping of this terrain was first done by the Geological Survey of India (e.g., references in Dasgupta et al. 2000; Basu 2013), and subsequent workers enriched it. The Tista Lineament: as per Fig. 3 of Mukul et al. (2014). MFT: Main Frontal Thrust, MBT: Main Boundary Thrust, RT: Ramgarh Thrust, RW: Rangit window, JT: Jorethang Thrust (after Bose et al. 2014), PT: Pelling Thrust, MCT: Main Central Thrust, DK: Darjeeling Klippe. Location names (red boxes): D: Darjeeling, Di: Dikchu, G: Gangtok, J: Jorethang, Ks: Kurseong, Ma: Martam, Pe: Pelling, Ph: Phamthang, R: Rabangla, Ru: Rumtek, S: Sevok, TB: Teesta Bazaar, Y: Yuksom. The blue boxes indicate Back-Structure Zones-A, B, C. Numbers (inside hexagons) associated with the earthquake epicenters represent their corresponding sl. no. as given in Supplementary Table 2. The inset stereonets show back-structure related attitudes of the Y- and P-planes, obtained in this study. **b** The duplex stacking in the Rangit window is to be noted. Reproduced from Fig. 1c of Parui and Bhattacharyya (2018). Cross-section drawn along Line-1 in **a**

related to the $F_1$ folds dip towards NNE (Gangopadhyay and Ray 1978), which means that the $F_1$ fold verges SSW and is a fore-fold. Sinha Roy (1973) provides sketches of conjugate folds/monoclinal warps with vergence towards 310° (~NW) from the metamorphic rocks of the Kalimpong hills in the DSH. Bhattacharya (1985) identifies four phases of folding from the Daling Group. The first two generations are coaxial, isoclinal, sometimes recumbent and are Precambrian "pre-Himalayan" events. Independent fieldwork by Ghose (2006) re-identifies these two generations of folds. Pyne and Gangopadhyay (1976) report two folding phases from the Buxa Group: $F_1$: minor but sufficiently penetrative tight to open doubly plunging folds; and $F_2$: local open puckers. Based on these, the authors, in their Fig. 8, interpret two S verging synclines with a possible S verging reverse fault plane in between as the regional structure. Such folds and faults are, therefore, fore-structures. Prakash and Tewari (2013) also report three deformation phases based on combined observations of the Daling schists (Lesser Himalaya) and the Paro gneisses (Higher Himalaya). Additionally, Bose et al. (2014) document a fourth phase of folding ($F_4$) that generated the orogen transverse regional folds. These authors also report that the regional structures in the DSH have been governed by the interference of the $F_3$ and the $F_4$ folds. The RT slipped the Daling Group and deformed quasi-plastically over the Gondwana/Buxa Formation in an elastic-frictional regime (Matin and Mazumdar 2009). From the microstructures of the garnet porphyroblasts, Saha (2013) predicted that the Sikkim LH underwent simple shear-dominated followed by pure shear-dominated deformation.

The MCT (recent review by Martin 2017a) activated in Sikkim multiply during 22, 14–15, 13 and 12–10 Ma (Catlos et al. 2004; Mottram et al. 2015), which was previously known to be grossly 23–10 Ma (Harris et al. 2004). The MCTZ is active even at present (Harris et al. 2004 and references therein) as also revealed by recent seismicity (De and Kayal 2004). The MCTZ, exhumed ~12 km (Harris et al. 2004) for 6.9 ± 3.7 Ma, underwent 42–73% simple shear (Ghosh and Bhattacharyya 2015) and also slipped right-laterally (De and Kayal 2004). The Higher Himalayan part of the Sikkim extruded through channel flow mechanism till 17–12 Ma and stopped before the LH started deforming (Searle and Szulc 2005).

## Metamorphism

The LH is metamorphosed dominantly to greenschist facies with chlorite and biotite grades (Dasgupta et al. 2004). Here the LH rocks gradually grade to MCTZ rocks of higher metamorphic grade through an inverted metamorphic sequence, whereas a structural discontinuity between them is missing (e.g., Lahiri 1973; Mohan et al. 1989; Dasgupta et al. 2004, Fig. 1 of Rubatto et al. 2013; Mottram et al. 2014a). The MCTZ rocks already reached the peak metamorphism prior to the main slip before 20 Ma (Mukhopadhyay et al. 2017). Prakash and Tewari (2013) link three phases of Lesser Himalayan deformations ($D_1$, $D_2$, $D_3$) with the two metamorphic phases ($M_1$, $M_2$) as follows: the regional greenschist facies prograde ($M_1$ early) metamorphism correlate with the $D_1$ deformation. This was followed by a regional-static-upper greenschist and amphibolite facies metamorphism ($M_1$ late) between the $D_1$ and the $D_2$ deformations. Finally, a lower-greenschist $M_2$ retrogression happened during the $D_2$ and the $D_3$ phases.

### Tectonics and seismicity

The MBT and the MCTZ merge at ~10 km depth with the Main Himalayan Thrust (MHT) dipping very gently towards N that defines a low-velocity zone (Acton et al. 2011). Thus, the Lesser Himalaya in Sikkim defines a crustal wedge. Reviewing its geometry and the kinematics, Mukul (2010) postulate a critical taper condition in the DSH. Chakraborty et al. (2017) in addition consider that the channel flow mechanism deformed the DSH. Fault plane solution and strong motion studies indicate that the MBT, a seismogenic and almost a mantle-reaching crustal fault (De and Kayal 2003), has a strike-slip component as well (Nath et al. 2005). Interestingly, the 6.9-Mw September 18, 2011 Sikkim Nepal seismicity too had a strike-slip component (Pradhan et al. 2013; Baruah et al. 2016). GPS studies indicate a ~0.4 mm $y^{-1}$ convergence rate for the Lesser Himalayan part of the DSH, as manifested by a flat topography (Mukul 2010). This might also be due to the fact that, in DSH transverse tectonics plays a key role in accommodating the India–Eurasia plate convergence (Hazarika et al. 2010). Out of several transverse features, the NW/NNW trending Tista Lineament (Fig. 2) passes through the study area along which several moderate earthquakes, landslides and strike-slip movements have taken place (Chakraborty et al. 2011; Dasgupta et al. 2013; Pradhan et al. 2013). Strike-slip tectonics has been one of the major mechanisms, besides fore-shear, for accommodating crustal shortening in the DSH (Hazarika et al. 2010). Details of few of the latest earthquakes have been compiled in Supplementary Table 2 and the corresponding epicenters are shown in Fig. 2. Review and original works on field structural geology was recently done around the Kurseong area by Banerjee et al. (2019).

### Ages and provenance

The U–Pb zircon thermochronology by Mottram et al. (2014b) shows that granites intruded the Lesser Himalayan host rocks before the injections in the Higher Himalaya. Presence of pre-Himalayan structural features and ~ 1850 Ma pegmatites that intruded in the Lesser Himalayan phyllites indicate Proterozoic magmatism at the northern boundary of the Indian plate (Acharyya et al. 2017). From $^{40}Ar/^{39}Ar$ dates of detrital white micas, Grujic et al. (2017) infer that the arkosic Gondwana rocks came from a Cambro–Ordovician (530–470 Ma) granite orogen through a southward sedimentary transport, whereas comparing the dates from the Namche Barwa and the Shilong Plateau, Martin (2017b) suggests the sources for these Gondwana sediments were the Kuunga- and the Pinjarra- orogens and a Neoproterozoic-Pleistocene Himalayan sequence. The Lingtse Gneiss klippes in the eastern part of the Lesser Himalaya were mainly pure sheared, followed by dominant simple-shear due to the presence of a lateral ramp (Das et al. 2016). Paul et al. (1996) report 1678 ± 44 Ma (Rb–Sr) and 1792 ± 45 Ma (Pb–Pb) ages for the Lingtse Gneiss.

## Field observations

Brittle shear sense was deduced based on the well-established concept that, from obtuse towards the acute angle between the Y- and the P planes is the shear sense (Fig. 6.3 of Mandl 2005; Fig. 5.50 of Passchier and Trouw 2005). We avoided possible cleavage refraction as shear sense indicator (Fig. 3a). An overall top-to-S/SW/SSW compressional brittle fore-shear has been documented from usually curved (sigmoid) P-planes bound by near-parallel Y-planes (Fig. 3b) as observed on road-cut ~ vertical rock-sections. Both the Y- and the P-planes have near similar strikes individually; their dips vary. While such top-to-S/W/SW Himalayan fore-thrusts exist profusely, back-structures were found only at fewer locations (GPS location of field-stops in Supplementary Table 3). The field locations presented in this chapter are distributed over the East Sikkim, South Sikkim and West Sikkim districts of Sikkim and the Darjeeling district of the West Bengal.

There are three major Back-Structure Zones (BSZs; locations marked by blue squares in Fig. 2) with top-to-N/NE brittle shear and NE verging folds from the Daling Group of rocks. The BSZ-A locate near the "*Damthang 3 km milestone*" near the locality Ravangla (location 15 in Fig. 2). Y-planes of back-structure cut those of the fore-structure (Fig. 4a) indicating the former to be younger. A few fore-sheared quartz veins also exist (Fig. 4b). Up to 6 cm-thick fault gouge zones exist along the planes of back-shear (Fig. 5). Even inside the fault gouge, back-structure P-planes develop locally. Such shear fabrics inside gouge have been reported earlier from other brittle shear zones (Mukherjee 2013b). Fault gouge dating can bracket absolute timing of this back-structure, but is outside the scope of this work.

The BSZ-B (Fig. 2 for location) develops near the *"Singtam District Hospital"* near the National Highway

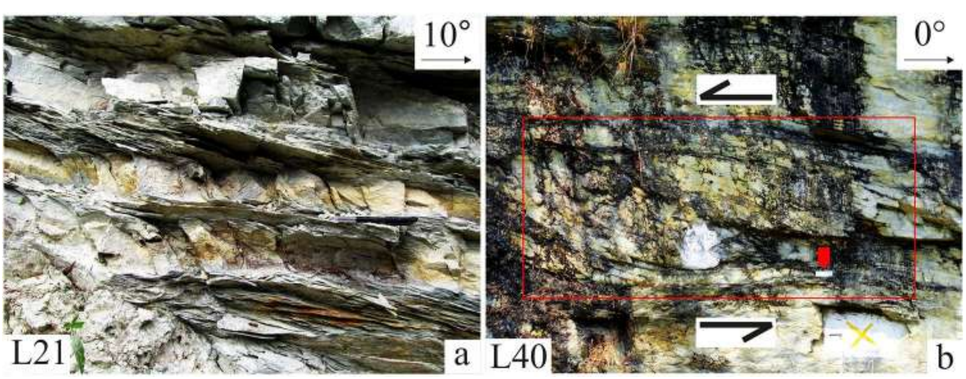


**Fig. 3** **a** Cleavage refraction in pelitic- and psammitic- schists of Daling Group, location 21 (27°23.806′N, 88°21.346′E) of Fig. 2a. Red arrowhead indicates the position of the 14 cm-long pen kept as a marker. **b** Brittle fore-structures: curvilinear fractures in Daling Group quartzites, location 40 (27°17.216′N, 88°18.416′E° of Fig. 2a. Red arrowhead indicates the position of the 15 cm-long scale kept as marker

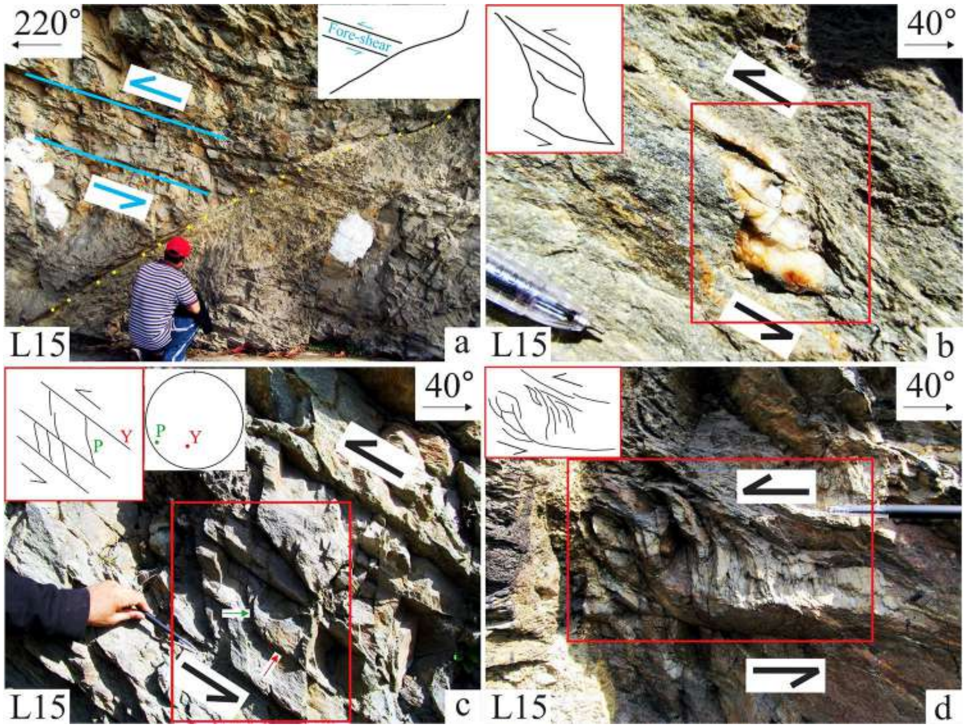


**Fig. 4** 'Back Structure Zone A', location 15 (27°14.676′N, 88°22.500′E) in Fig. 2a. Fore-structures present in psammitic schists of Daling Group. **a** Truncation of fore-structure: Y-planes (blue parallel lines) against the back-shear Y-plane (yellow broken line). Mukherjee ~ 80 cm height in seated position, as a marker. **b** Sigmoid quartz vein shows fore-shear. Notice nearby unsheared quartz veins. ~ 4 cm portion of *a* pen is visible, as a marker. **c** Fore-shear documented by brittle Y- and P- planes. Y-plane attitude: 105°/45° → 15° (strike/dip → dip direction; measured at the red arrow). P-plane attitude: 150°/78° → 60° (measured at the green arrow). Poles of the Y-, P-planes are plotted in the inset stereonet. Red rectangle indicates the part sketched in the inset diagram. ~ 14 cm-long pen as scale. **d** Brittle fore-shear documented by non-parallel Y-planes that bound sigmoid P-planes. ~ 10 cm-long pen as a scale

31A. Along with the brittle Y- and P- planes (Fig. 6a–c), brittle shear is also revealed by a single back-fold (Fig. 6d). The fold is a SW vergent round hinge isoclinal synform with sub-horizontal fold axis and SE-dipping limbs. This possibly indicates that the back-deformation started while the host rock was in a deeper ductile regime and the same pattern of deformation continued in the shallower brittle domain, the terrain being under the same ~ NE-SW compression regime of India–Eurasia collision. The BSZ-C is ~ 200 m-long exposure near the village Kyongsa close to the "*Geyzing 2 km/Pelling 7 km milestone*". As in BSZ-B, back-folds also occur here but only few deformed quartz veins exist (Fig. 7).

Besides the three BSZs, sporadic back-structures have also been noted at several other locations (Figs. 8, 9, 10, 11; Fig. 2 for locations). Kink folds with moderate to low dipping axial planes exist in a few locations (Fig. 12), but are not reliable shear sense indicators (Mukherjee et al. 2015). Since back-structures are observed only at the surface, their extent and geometries below the surface remain indeterminate. Supplementary Fig. 1 plots the attitudes of the Y- and the P-planes indicating fore- and back-shears.

## Discussions: focus on genesis of back-structures

Following the standard procedure of interpreting shear senses in shear zones, we have interpreted sheared veins (also see for similar approach Fig. 10 of Hodgson 1989; Koehn and Passchier 2000; Mukherjee 2014, 2015). Tectonic or large-scale deformation implications of small-scale veins have been reviewed and discussed in detail by Bons et al. (2012; also see Montomoli et al. 2005).

Based on (i) the structural data we gathered in the field (e.g., stereoplots in Fig. 2), and (ii) plotting their locations on the map (red second brackets in Fig. 2b), it is understood that the sample locations all come from a nearly unidirectional dipping lithounits. Therefore, we conclude that the different shear senses (back thrusts) encountered in the study area are not because any effect of regional folding.

Several cross-sections drawn across the Himalayan strike at different locations by different authors have shown the same structures such as the MCT and the STD. Lack of geophysical data at this moment precludes us to

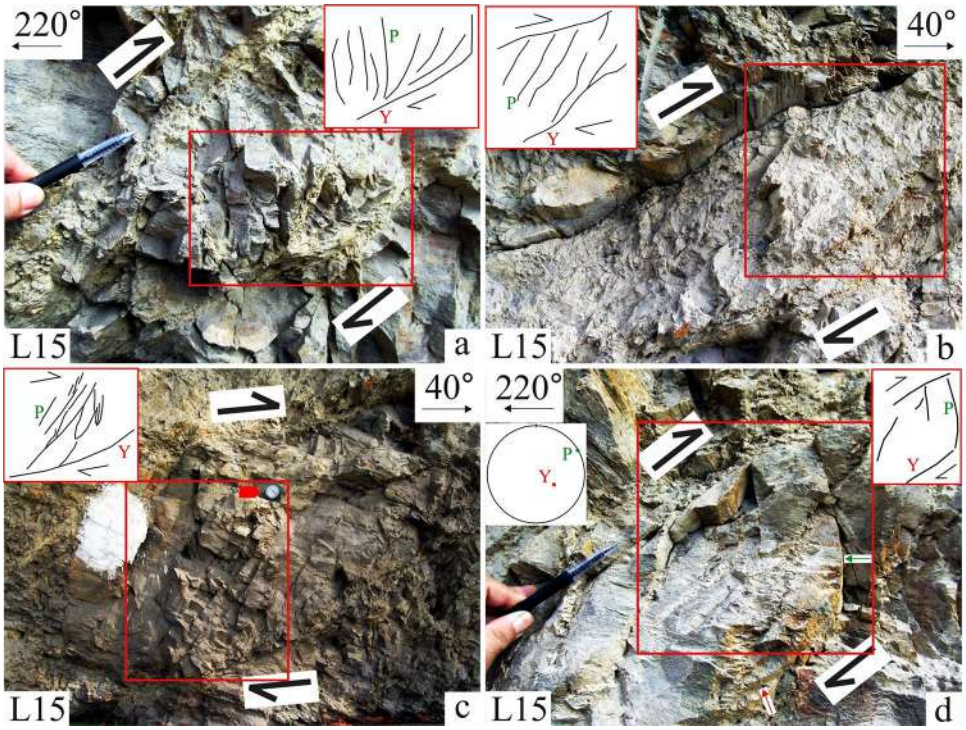


**Fig. 5** 'Back Structure Zone A', location 15 (27°14.676′N, 88°22.500′E) of Fig. 2a. Back-structures present in psammitic schists of Daling Group. **a** Back-shear represented by brittle Y- and sigmoid P-planes. Fault gouge in the fractures. ~6 cm portion of a pen as a scale. **b** Back-sheared fault gouge (width of view ~1.5 m). Red rectangle indicates the part sketched in the inset diagram. Width of exposure ~3 m. **c** Curved P-planes of back-shear. Red arrowhead indicates the position of a clinometer kept as a scale. Length of the bridge of clinometer is ~8 cm. **d** Fault gouge preserved in the brittle Y- and P-planes of back-thrust. (The plane photographed is a sub-vertical plane with ~87° dip). Y-plane attitude: 30°/35°→300° (measured at the red arrow). P-plane attitude: 150°/88° (measured at the green arrow). Poles of the Y-, P-planes are plotted in the inset stereonet. ~7 cm portion of a pen as the marker

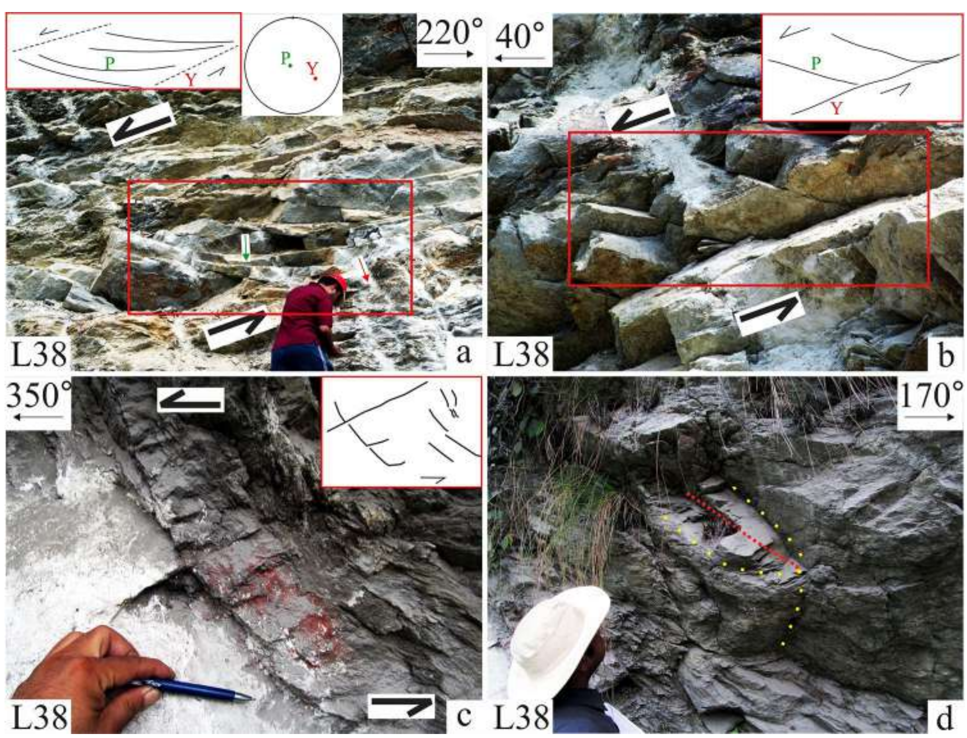


**Fig. 6** 'Back Structure Zone B', location 38 (27°13.717′N, 88°29.627′E) in Fig. 2a. Back-structures present in psammitic schist of Daling Group. **a** Back-structure defined by Y- and P-structures. Y -plane attitude: 30°/45°→120° (measured at the green arrow), P-planes curved, sub-horizontal (measured at the green arrow). Poles of the Y-, P-planes are plotted in the inset stereonet. Mukherjee (*waist to head~80 cm height*) as a scale. **b** Another back-structure similar to the previous figure. Width of exposure~2 m. **c** P-plane of a back-structure. The high-angle fractures associate with it. ~8 cm portion of a pen as a scale. **d** An isoclinal-overturned-synformal back-fold. Northern limb dips 60° towards 115°. N. Bose, ~30 cm in the photograph, as a scale

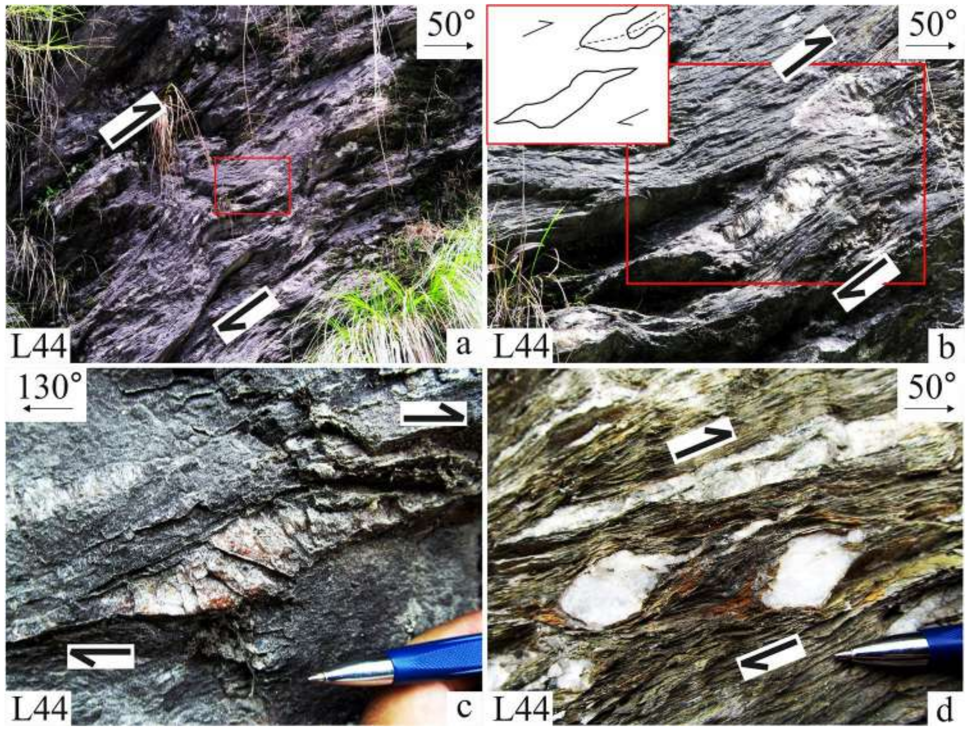


**Fig. 7** 'Back Structure Zone C', location 44 (27°17.721′N, 88°14.784′E) in Fig. 2a, ductile shear found. Back-structures present in schists of Daling Group. **a** Sheared quartz veins enveloped by undulating Y-planes indicate back-shear. Width of exposure ~ 2 m. **b** A part of previous figure (inside red rectangle) zoomed. Notice the sigmoid quartz veins and the NE-vergence of the folded quartz vein (top right). **c** Sigmoid shaped quartz vein showing top-to-50° shear. ~ 8 cm portion of a pen as a scale. **d** Two quartz sigmoids: left one is almost orthogonal showing no shear, the right one *shows* a top-to-right sense of shear (i.e., back-shear). Few quartz veins are not sheared. ~ 4 cm portion of the pen as a scale

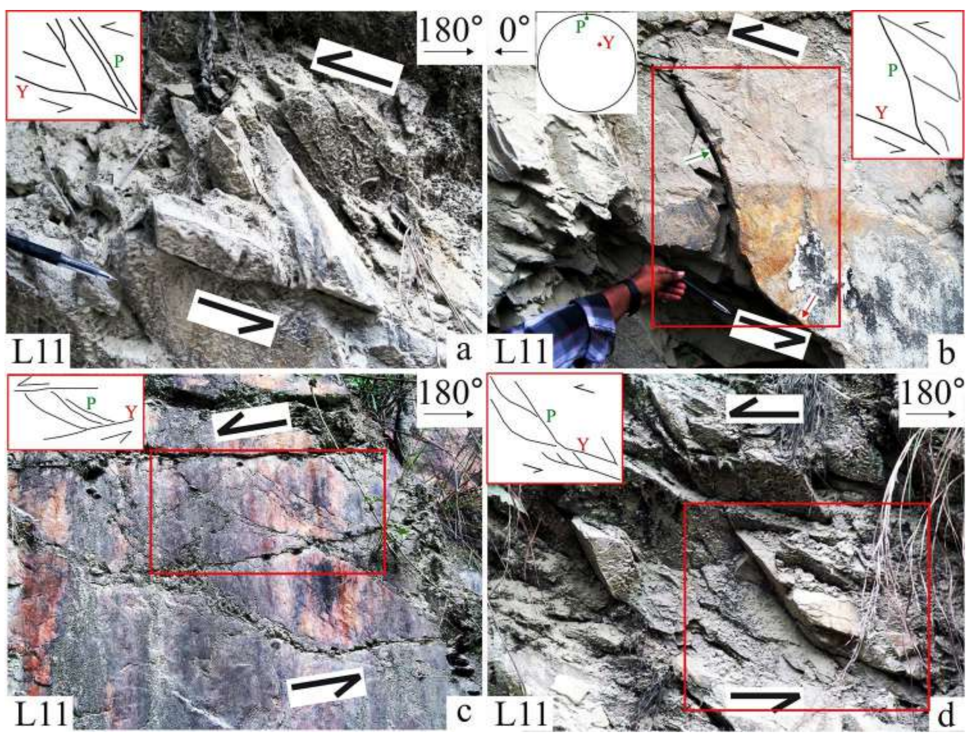


**Fig. 8** Back-structures found at locations other than the Back-Structure Zones *A, B, C*. Location 11 (26°06.305′N, 88°21.738′E) in Fig. 2a. Back-structures present in psammitic quartzite of Daling Group. **a**–**d** Back-structures present as Y- and P-planes. Both straight and curved P-planes are to be noticed. **a** ~ 8 cm portion of a pen as a scale. **b** Y-plane attitude: 125°/38° → 215° (measured at the green arrow), P-plane attitude: 90°/80° (measured at the green arrow). Poles of the Y-, P-planes are plotted in the inset stereonet. A ~ 14 cm-long pen as a scale. **c** Width of exposure ~ 3 m. **d** Width of exposure ~ 2 m

extrapolate back structures at depth, and, therefore, we cannot bring out the exact geometry of the back-structures at depth and in cross-sections. The back structures we report occur many times inside a single lithology and not at well-known lithological interfaces. If the latter were the case, one could have extrapolated the back-structures coincident with the litho-contact and in that way predict the sub-surface disposition of structures in the existing cross-sections where that litho-contact is already drawn.

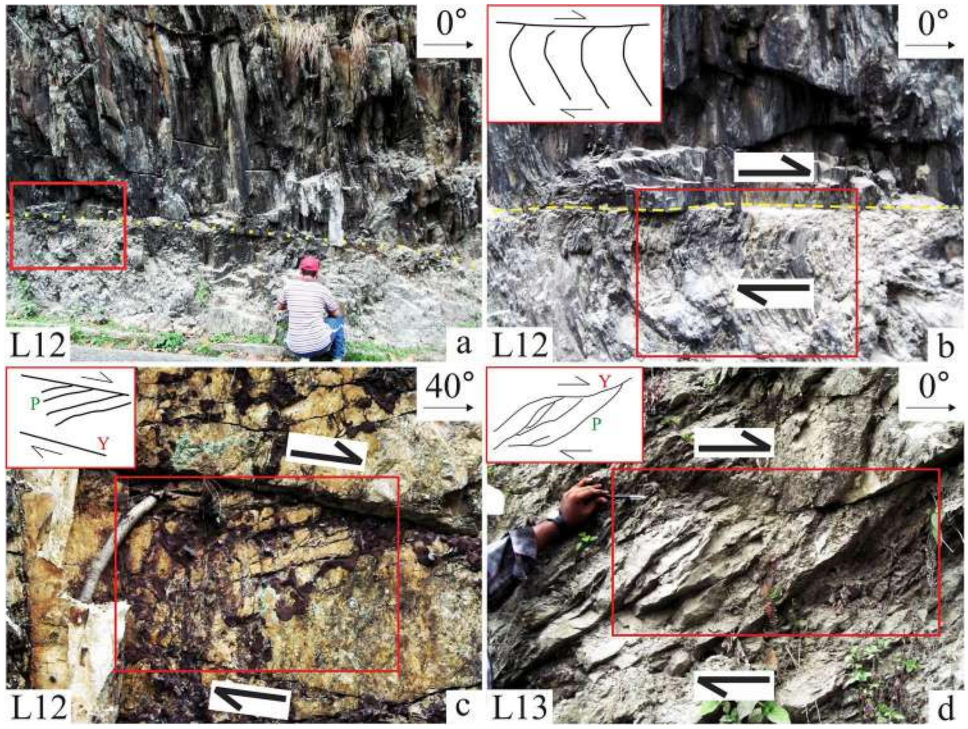


**Fig. 9** Discrete back-structures: **a** sub-horizontal discontinuity (yellow broken line) separates deformed lower part from the relatively undeformed upper part. Shale of Daling Group, location 12 (27°06.366′N, 88°21.587′E) in Fig. 2a. Mukherjee in seated position, ~ 80 cm height, as a scale. **b** Red box in previous figure zoomed. Drag fold (Mukherjee 2014) in the lower part indicates a back-shear along the discontinuity. **c** Brittle Y- and P-planes show back-shear. Quartzite of Daling Group, location 12 (27°06.366′N, 88°21.587′E) in Fig. 2a. Width of exposure ~ 2 m. **d** Anastomosing sigmoid fractures define P- planes and reveal back-shear. Phyllites of Daling Group, location 13 (27°09.017′N, 88°20.917′E) in Fig. 2a. A ~ 14 cm-long pen as a scale

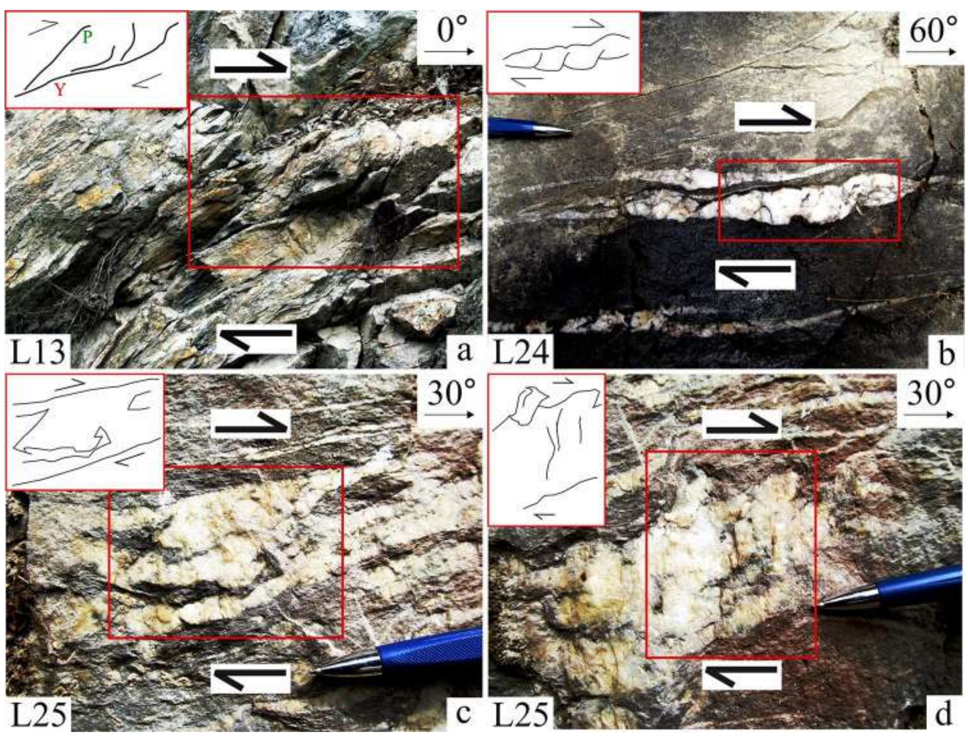


**Fig. 10** Discrete back-structures: **a** curved Y- and P-planes show back-shear. Phyllites of Daling Group, location 13 (27°09.017′N, 88°20.917′E) in Fig. 2a. Width of exposure ~ 2 m. **b–d** Ductile sheared quartz veins show back-shear. Unsheared quartz veins. Psammitic schists of Daling Group. ~ 5 cm length of a pen as a scale. **b** Location 24 (27°16.422′N, 88°22.076′N) in Fig. 2a. **c**, **d** Location 25 (27°16.172′N, 88°21.915′E) in Fig. 2a

Millimeter- to centimeter-scale displacements along shear planes documented in a single terrain over a large spatial extent can cumulatively give rise to kilometers of slip in shear zones (Jain and Manickavasagam 1993; Hubbard 1996; re-referred in Mukherjee and Koyi 2010a). Shear zone structures are fractal (Sammis and Steacy 1995) and large-scale manifestation of small-scale structures such as brittle faults should exist in the field. However, since the studied rock exposures are almost always vertical to sub-vertical, we could not apply Google Earth images to locate any

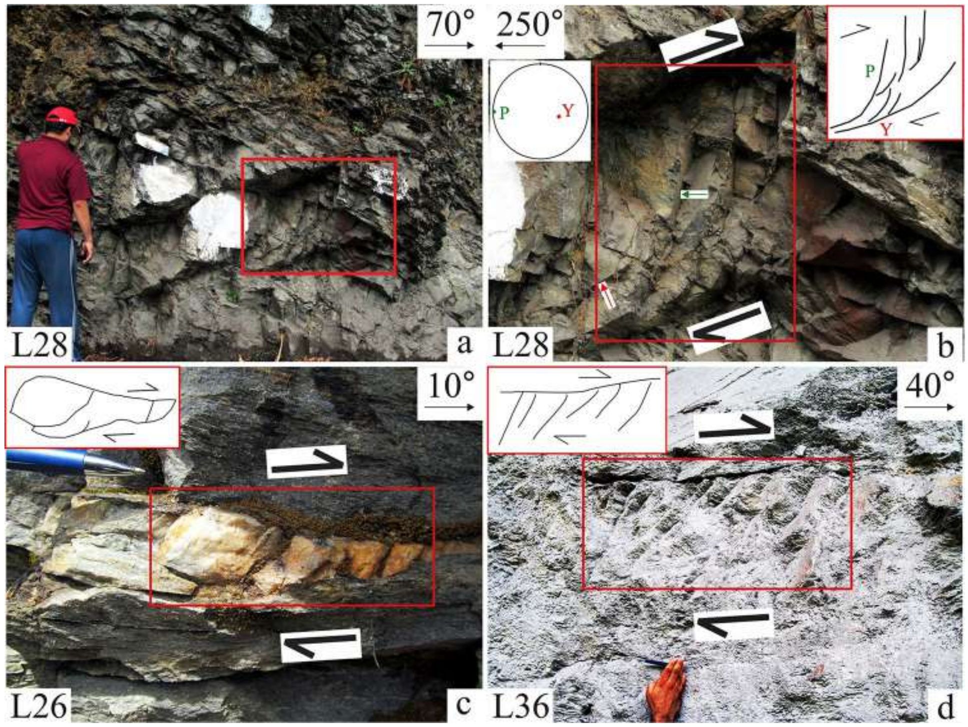


**Fig. 11** Discrete back-structures: **a** defined by Y- and P-planes (red box) inside a zone of fore-structures in psammitic schists of Daling Group, location 28 (27°14.988′N, 88°23.933′E) in Fig. 2a. Mukherjee with ~ 165 cm height as a scale. **b** Red-boxed part of previous figure zoomed. P-planes curved. Y-plane attitude: 15°/33° → 285° (measured at the green arrow). P-plane attitude: 0°/88° (measured at the green arrow). Poles of the Y-, P-planes are plotted in the inset stereonet. **c** Back-sheared quartz vein, schists of Daling Group, location 26 (27° 15.932′ N, 88° 22.159′ E) in Fig. 2a. ~ 5 cm length of a pen as a scale. **d** Discrete back-structure defined by Y- and P- planes. Lingtse Geneiss of Daling Group, location 36 (27° 15.826′ N, 88° 34.234′ E) in Fig. 2a. ~ 10 cm portion of a pen as a scale

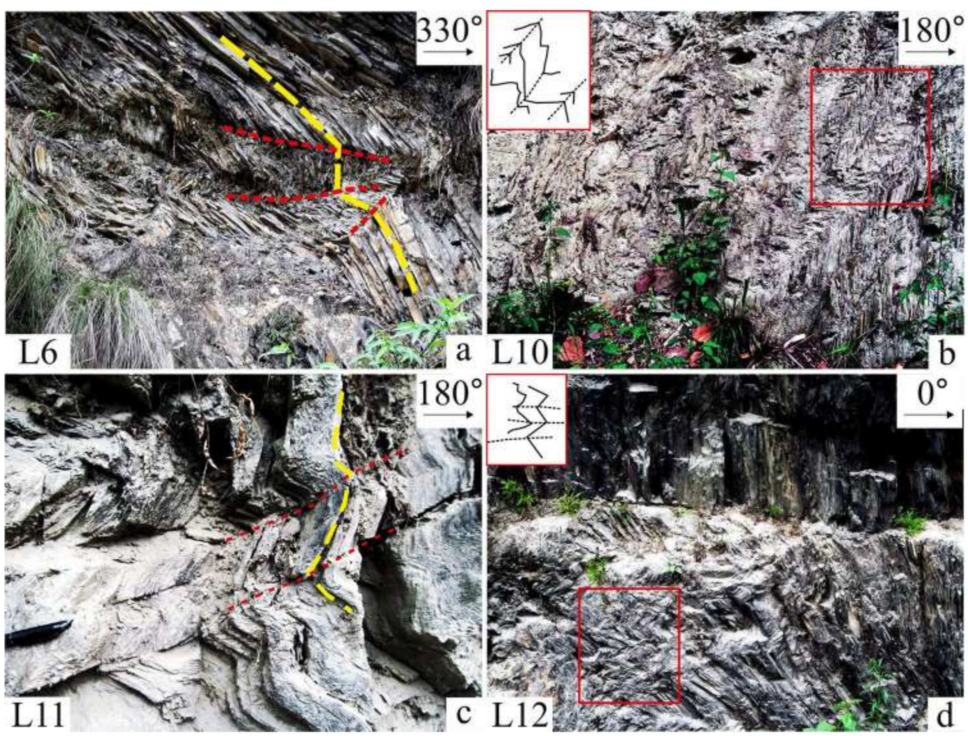


**Fig. 12** Kink folds: **a** Daling Group shales, location 6 (27°00.985′N, 88°26.110′E) in Fig. 2a. Width of exposure ~ 4 m. **b** Daling Group shales, location 10 (27°05.541′N, 88°23.723′) in Fig. 2a. Width of exposure ~ 3 m. **c** Daling Group psammitic schists, location 11 (26°06.305′N, 88°21.738′E) in Fig. 2a. Fracture planes are sub-parallel to the axial plane of the fold. ~ 5 cm length of a pen as a scale. **d** A sub-horizontal shear plane separates deformed (kinked) lower part from the relatively undeformed upper part. Shales of Daling Group, location 12 (27°06.366′N, 88°21.587′E) in Fig. 2a. Width of exposure ~ 3 m. The folded layers and axial traces have been sketched. Red rectangles in **b**, **d** show the parts which have been sketched in the inset diagrams

large-scale faults. Further, limited exposures were observed in those sections because of the specific mountain terrain that is partly covered by landslides and partly by vegetation. In summary, although we did not document large-scale faults, repeated occurrence of small-scale structures with a specific attitude (refer attitude info here for the Y-plane in the three zones BSZ-A, B and C) connotes its large-scale implication. Note that in no single exposure the entire or even a partial exposure of the Himalayan cross-section (e.g., Fig. 2a of Iaccarino et al. 2016) has been understood.

Previous authors have recognized thrusts structurally purely based on meso- and micro-scale observations (e.g., the High Himal Thrust through Fig. 2a–d in Montomoli et al. 2015). Rather the information has been compiled based on surface observations by geologists and sub-surface studies by geophysicists. Likewise, none has “seen” the parabolic velocity profile for a crustal channel flow in the Greater Himalayan Crystallines. It is rather interpreted so based on small-scale observations, and sometimes coupled with geochronologic data (e.g., Mukherjee and Koyi 2010b). Montomoli et al. (2015) documented a km-scale thick mylonite zone and deciphered the deformation to be distributed and, therefore, having a tectonic implication. In our case, we note back-shears as isolated exposures and in smaller scale having nearly the same N/NE vergence from a very vide transect. This means that the deformation is regionally extensive and, therefore, must have a tectonic connotation.

The prerequisites of back-thrust generation, such as brittle rheology and fault bends (Xu et al. 2015 and references therein) match with the geological setting in this study area. The fault bend in the present case is the ramp and flat structure produced at ~ 10 km depth by the stacking of the Lesser Himalayan duplexes (Fig. 2b). This section will link field observations of the present study with the previously proposed models of back-structures. All these models are the different versions of critical taper mechanism. The present field study cannot pin-point whether one single of these or several of the factors of back-structures operated in the Sikkim Lesser Himalaya. Further, what mechanism guides back deformation in other segments of the Himalaya, e.g., the Siwalik range and the Greater Himalayan Crystalline, would require separate field-based studies coupled with analogue/analytical models.

## Classical critical taper mechanism (Fig. 13a)

At the convergent plate boundary with a critical taper setting, the ‘hard’ backstop, equivalent to the Eurasian plate in our case, acts as a strong barrier, in front of which the ‘weaker’ foreland materials of Indian crust accumulates on the subducting plate due to collision-induced crustal shortening. Due to this strength contrast and the velocity of the subducting plate, the frontal part of the accretionary wedge undergoes back-thrusting (Fig. 1 of Xu et al. 2015). Here back-thrusting takes place along the contact between the foreland-ward dipping backstop and the accretionary prism (Fig. 13a). Such thrusts can generate either in the frontal part of the Lesser Himalayan wedge, or near the back-stop. The later position is the suture zones in the Himalayan context. In the map of the Rangit Window, Bhattacharyya and Mitra (2009) plotted four closely spaced S-dipping thrusts named-Jorethang, Sorok, Kitam and Ramgarh Thrusts. Hence these thrusts act as back-thrusts in this part. Interestingly, Ghosh et al. (2016) report shear intensification at Daling Thrust and their Fig. 2b shows a back-thrust named the Jorethang Thrust (plotted in Fig. 2a). Furthermore, Ghosh et al. (2018) provide a field-example of back-thrust from the frontal part of the Darjeeling-Sikkim Lesser Himalaya and their analog modeling also shows generation of back-thrusts at the frontal part of the crustal wedge. The locations 11–13 of this study (Fig. 2a for location) are very close to this back-thrust. Hence, the back-structures seen at those locations can be correlated to their mechanisms, i.e., duplexing and strain intensification.

## Sub-surface barriers like ramp/thrust bend (Fig. 13b)

The velocity of thrust sheet usually decreases while overriding a rampor a thrust bend. Thus, rocks compress more at the toe of the ramp (Fig. 8 of Little 2004). In such a scenario, back-thrusts develop in the thrust sheet present above the ramp. As a consequence, the base of the ramp would release the accumulated strain (Xu et al. 2015, Fig. 13b). Presence of < 10 km deep sub-surface ramps or bends (created by duplex stacking) along faults/shear planes is also common in our study area (Fig. 6 of Mitra et al. 2010). In this study, we found three BDZs and six other back-shear locations on the northern side of the anticlinal duplex stack (map: Fig. 2). In this part, several thrust bends and ramps are present (Fig. 6 cross-section of Bhattacharyya and Mitra 2009). So, the observed back-structures can be correlated with this model.

## Wedging, passive roof duplexing (Fig. 13c)

Wedge-shaped crustal slices, enveloped by a pair of opposite verging non-parallel faults, a fore-thrust and a back-thrust-are common in collisional orogens. The opposite-dipping faults meet at sub-surface constituting the tip of the wedge defining a “flake structure” (Fig. 1 of Oxburgh 1972) or a ‘seismic crocodile’ (Fig. 2b of Meissner 1989). During collisional compression, the tip of the wedge moves further towards foreland by delaminating the crust. This foreland-ward propagation of the crustal wedge is accompanied by a system of passive roof duplexing (Banks and Warburton 1986; Avé Lallemant and Oldow 1998) whereby the mountain front/foreland side shortens. This antiformal stack of duplexes has an almost static overlying sequence, which is separated by a sub-horizontal roof thrust. While the thrust propagates by antifomal piggy-back stacking of the underlying duplex horses, the roof sequence slices may imbricate and erode to maintain equal lengths of the beds on either side of the roof thrust (Fig. 13c). Thus, while the wedge moves actively towards foreland, the overlying sequence moves passively towards the hinterland (Figs. 6 and 7 of Banks and Warburton 1986). A zone of back-shear develops

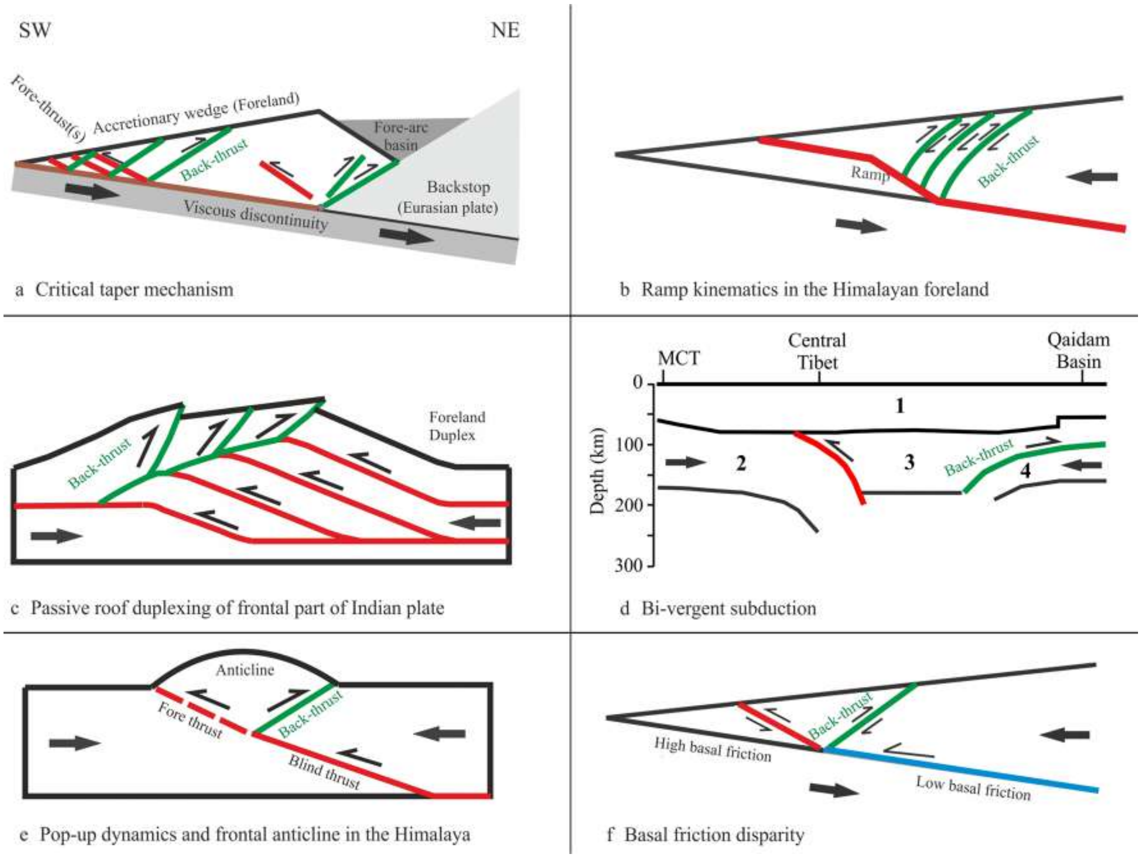


**Fig. 13** Geneses of back-structures in the collisional orogen such as the Himalaya. Right-hand side is north geographic direction. Schematic diagrams, not to scale. In all the sub-figures, right-hand side indicates north-east direction if these concepts are to be matched with this study. **a** Components of a critical taper and back-thrusts at the fore-arc region (redrawn after Fig. 1 of Xu et al. 2015). **b** Strain accumulation and back-thrusting at a frontal ramp/fault bend (redrawn after Type I in Fig. 2a of Xu et al. 2015). **c** Passive roof duplex (redrawn after Fig. 7 of Banks and Warburton 1986) mechanism back-thrusts. **d** Example of "bi-vergent subduction" (redrawn from "East Line" in Fig. 4 of Zhao et al. 2010). 1—undifferentiated India–Eurasia crust, 2—Indian mantle lithosphere, 3—crush zone, 4—Asian mantle lithosphere. **e** Blind thrust model for the origin of frontal anticlines. Movement along the back-thrust and fore-thrust (both originated from the tip of blind thrust) generates flexure slip fold as the pop-up structure (redrawn after Fig. 4b of Schultz 2000). **f** Back-thrusting associated with an increase in friction along the decollement (redrawn after Fig. 2a of Xu et al. 2015)

along the contact of the overlying sequence and the wedge. Back deformation overcomes the space problem arising due to the backward rotation of beds and foliation planes present in the duplexes. Zuppetta and Mazzoli (1997) supported the idea of 'passive roof duplex' while describing the origin of the out-of-sequence back-thrusts and back-folds present at the southern Apennines thrust and fold belt, Italy. The sizes of the wedges can range microscopic up to plate-scale (Price 1986). In the Darjeeling–Sikkim Himalaya, the Lesser Himalaya is duplexed intensely. Therefore, the 'passive roof duplex' model is another possibility of the back-thrust mechanism here, as also seen in field (Fig. 9a, b).

## Relation with back-folds

Back-folds (Fig. 1e) originate in deeper ductile regime unlike the brittle back-thrusts at the shallower depth (Avé Lallemant and Oldow 1998). In our study, few back-folded quartz veins (Fig. 7) are noted inside the psammitic schist (for detailed field observations see 'BSZ-C' in Sect. 3). The low-metamorphic-grade of such a country rock does not indicate that they were exhumed from the ductile regime of the crust. Rather they were exhumed from much shallower brittle regime. From magnetic studies, Tiwari et al. (2006) proposed a ~ 12 km deep detachment for Sikkim Lesser Himalaya. In this scenario, the genesis of the folded quartz veins can be explained by the mechanism proposed by Trepmann and Stöckhert (2009). From micro-structural analyses, those authors concluded that the contrast in effective viscosity between host meta-greywacke and quartz veins led to the folding of the veins during a continuous high-stress deformation at a rather low temperature of 250–300 °C. Hence, the back-folds observed in our study (Fig. 7) are related to shallow-level back-deformations in brittle regime.

## Other potential causes

These mechanisms might be valid in other Himalayan sections, but at the current state of knowledge, they cannot be directly linked with the field observations presented in this study.

### Bi-vergent subduction (Fig. 13d)

Tectonic wedging of larger scales may lead to bi-vergent shear and folding at the collisional plate boundaries (Fig. 19 of Price 1986). Back-thrusting in collisional terrains can be due to a reversal in subduction direction (Review of Kroehleret al. (2011). Zhao et al. (2010) presented India–Eurasia subduction scenario from four seismic sections across the Himalayan orogen. They report such tectonic wedge(s) in the central- and the eastern- Himalaya (Figs. 1 and 4 of Zhao et al. 2010). Backthrusts documented in the field within the entire Lesser Himalaya (Sikkim) locate nearly equidistant from their "central line" and the "eastern line". Cross-section along the central line does not show the presence of the Asian mantle lithosphere. However, geophysical information from the eastern line connotes the Asian mantle lithosphere subducts ~ 170 km deep towards S. Whether this subduction plays any role in generating back-structures in the Himalaya needs to be checked. The explanation resembles the interpretation of back-structures observed in Bhagirathi section of the Higher Himalaya in Uttarakhand, India, as per Mukherjee (2013b).

### Blind fault and pop-up structure

Significant strain accumulates in the fault zones when one faulted block stops against the other, while the former remains stressed ("stick" component of the "stick–slip mechanism"). The stored energy is manifested eventually by conjugate faulting- one fore-thrust and the other a back-thrust-together constituting a pop-up structure from the tip of the terminated fault (Type III in Fig. 2a of Xu et al. 2015). While presenting a new model for the origin of wrinkle ridges, Schultz (2000) proposed that the conjugate back- and fore-thrusts produce flexure slip anticlines in the overlying beds of the blind thrust (Fig. 13e).

Back-thrust-induced back-folds can form in the hanging-wall of the thrust plane (Zuppetta and Mazzoli 1997). Price (1986) viewed differently such back-folds as a part of multiphase orogeny. Anticlinal back-folds (similar to fault-propagation folds) can generate atop blind back-thrusts (Fig. 13e). Such a mechanism generated frontal anticline near the Main Frontal Thrust at the Kashmir Himalaya (India, Fig. 1 of Vassallo et al. 2015). A regional frontal anticline is present in the LHS near the Main Boundary Thrust in Sikkim (Fig. 2). The Main Frontal Thrust too is blind in this part of the Himalaya (e.g., Mukul 2000). Therefore, pop up structure-related blind faulting could generate back deformation in our study area.

### Basal friction anomaly (Fig. 13f)

In addition to a tectonic wedge sliding in geological time over a basal detachment, friction increases towards the toe of the wedge along the fault. An inhomogeneous fault zone with materials of different strength will have variable friction (Luo and Ampeuro2018). Where higher friction develops on the thrust, the thrust sheet retards (Type II in Fig. 2a of Xu et al. 2015). Here, the thrust sheet strains more at the zone of retardation and back-deforms to release the stored energy (Cubas et al. 2013a, b and refs. therein). A very high conductive zone of 2–5 Ω-m at ~ 3–15 m depth documented N to MBT in the Sikkim Lesser Himalaya may indicate the presence of fluids (Patro and Harinarayana 2009). This can reduce the friction for brittle faulting. Thus we consider basal friction anomaly as a potential reason for back-thrusting in Sikkim Lesser Himalaya.

## Conclusions

In this study we document back-structures (meso-scale back-thrusts in ductile and brittle regimes and back-folds) from the Sikkim Lesser Himalaya. Along with several other back-structure locations, three Back-Structure Zones (long stretches with intense back-structures) have been identified. Considering back-thrusting and -folding to be scale-independent, their mechanisms have been correlated with the field observations, to understand the genesis of the structures. Evidences for the back-structure mechanisms such as critical taper, passive roof duplex and ramp-related models have been provided and other potential models have been discussed. Competency contrasts with the host rock back-folded the quartz veins. This study works as a stepping stone for many subsequent studies, such as- micro-structural investigations to understand the stress–strain conditions for the generation of back-structures, relative-/absolute- ages of the back-structures and their role in the deformation history, etc.

The ductile back-structures were presumably produced before the brittle back structures. It could mean that the extruding rock in the Lesser Himalaya was activated by first the ductile backstructures, and it was then followed by the brittle backstructures. Whether backstructures altered the metamorphic evolution of the terrain could be matter of future research.

We also documented backstructures from another transect from the Garhwal Lesser Himalaya (Bose and Mukherjee 2019), which means that such structures developed mainly as distinct zones at several places in the Lesser Himalaya.

Focused fieldworks on Lesser Himalaya along other river sections might prove that the back-structures are the integral part of the Lesser Himalayan tectonics.

**Acknowledgements** We thank IIT Bombay for funding the 2014 Sikkim fieldwork. The fieldwork in 2015 was funded by NB's UGC Fellowship: F.2-2/98(SA-1). Feedback received from 30th Himalaya Karakoram Tibet Workshop (Dehradun, India) through NB's poster presentation has been beneficial. Several comments by K. Pande and G. Mathew (Research Policy Committee, IIT Bombay), and S.G. Gokarn (retired from Indian Institute of Geomagnetism) kept NB alert. Positive detail critical reviews in two rounds provided by Rodolfo Carosi (University of Torino) and in a single round by Joyjit Dey (Leeds University) are acknowledged. Wolf-Christian Dullo and Monika Dullo are thanked for punctual editorial handling.

## References

Acharyya SK, Ghosh S, Mandal N, Bose S, Pande K (2017) Pre-Himalayan tectono-magmatic imprints in the Darjeeling–Sikkim Himalaya (DSH) constrained by $^{40}$Ar/$^{39}$Ar dating of muscovite. J Asian Earth Sci 146:211–220

Acton CE, Priestley S, Gaur VK (2011) Crustal structure of the Darjeeling–Sikkim Himalaya and southern Tibet. Geophys J Int 184:829–852

Agarwal A, Agarwal KK, Bali R, Prakash C, Joshi G (2016) Back-thrusting in Lesser Himalaya: evidences from magnetic fabric studies in parts of Almora crystalline zone, Kumaun Lesser Himalaya. J Earth Syst Sci 125:873–884

Avé Lallemant HG, Oldow JS (1998) Antithetic shear and the formation of back-folds in the central Brooks Range fold and thrust belt, Alaska. In: Oldow JS, Ave Lallemant HG (eds) Architecture of the Central Brooks Range fold and thrust belt, Arctic Alaska. Geol Soc Am Spec Pap 324:253–259

Banerjee S, Bose N, Mukherjee S (2019) Field structural geological studies around Kurseong, Darjeeling–Sikkim Himalaya, India. In: Mukherjee S (ed) Tectonics and structural geology: Indian context. Springer, Berlin, pp 425–440. ISBN: 978-3-319-99340-9

Banks CJ, Warburton J (1986) 'Passive-roof' duplex geometry in the frontal structures of the Kirthar and Sulaiman mountain belts. Pak J Struct Geol 8:229–237

Baruah S, Saikia S, Baruah S, Bora PK, Tatevossian R, Kayal JR (2016) The September 2011 Sikkim Himalaya earthquake Mw 6.9: is it a plane of detachment earthquake? Geomat Nat Hazards Risk 7:248–263

Basu SK (2013) Geology of Sikkim and Darjeeling District of West Bengal. Geological Society of India, Bangalore

Bhattacharya NC (1985) Geology and mineralization of Pedong-Pshok area with a discussion on the nature and origin of the Lingtse granite gneiss, Darjeeling district, West Bengal and Sikkim. Indian Mineral 39:61–78

Bhattacharyya K, Ahmed F (2016) Role of initial basin width in partitioning total shortening in the Lesser Himalayan fold-thrust belt: insights from regional balanced cross-sections. J Asian Earth Sci 11:122–131

Bhattacharyya K, Mitra G (2009) A new kinematic evolutionary model for the growth of a duplex—an example from the Rangit duplex, Sikkim Himalaya, India. Gondwana Res 16:697–715

Bons P, Elburg MA, Gomez-Rivas E (2012) A review of the formation of tectonic veins and their microstructures. J Struct Geol 43:33–62

Bose N, Mukherjee S (2019) Field documentation and genesis of the back-structures from the Garhwal Lesser Himalaya, Uttarakhand, India. In: Sharma R, Villa IM, Kumar S (eds) Crustal architecture and evolution of the Himalaya–Karakoram–Tibet Orogen, vol 481. Geological Society, London, Special Publications. https://doi.org/10.1144/SP481-2018-81

Bose S, Mandal N, Acharyya SK, Ghosh S, Saha P (2014) Orogen-transverse tectonic window in the Eastern Himalayan fold belt: a superposed buckling model. J Struct Geol 66:24–41

Butler RWH, Mazzoli S, Corrado S, DeDonatis M, Di Bucci D, Gambini R, Naso G, Nicolai C, Scrocca D, Shiner P, Zucconi V (2004) Applying thick-skinned tectonic model to the Apennine thrust belt of Italy—limitations and implications. In: McClay KR (ed) Thrust tectonics and hydrocarbon systems. Am Assoc Pet Geol Mem 42:647–667

Buttinelli M, Improta L, Bagh S, Chiarabba C (2016) Inversion of inherited thrusts by wastewater injection induced seismicity at the Val d'Agri oilfield (Italy). Sci Rep 6:37165. https://doi.org/10.1038/srep37165

Carmignani L, Carosi R, Di Pisa A, Gattiglio M, Musumeci G, Oggiano G, Carlo Pertusati P (1994) The hercynian chain in Sardinia (Italy). Geodin Acta 7:31–47

Carosi R, Montomoli C, Iaccarino S, Massonne HJ, Rubatto D, Langone A, Gemignani L, Visonà D (2016) Middle to late Eocene exhumation of the Greater Himalayan Sequence in the Central Himalayas: progressive accretion from the Indian plate. Geol Soc Am Bull 128:1571–1592

Carosi R, Montomoli C, Iaccarino S (2018) 20 years of geological mapping of the metamorphic core across Central and Eastern Himalayas. Earth Sci Rev 177:124–138

Catlos EJ, Dubey CS, Harrison TM, Edwards MA (2004) Late Miocene movement within the Himalayan Main Central Thrust shear zone, Sikkim, north-east India. J Meta Geol 22:207–226

Chakraborty I, Ghosh S, Bhattacharya D, Bora A (2011) Earthquake induced landslides in the Sikkim-Darjeeling Himalayas—An aftermath of the 18th September 2011 Sikkim earthquake. Geology Survey of India (Engineering Geology Division), Eastern region, Kolkata, pp 1–8

Chakraborty S, Mukhopadhyay DK, Chowdhury P, Rubatto D, Anczkiewicz R, Trepmann C, Gaidies F, Sorcar N, Dasgupta S (2017) Channel flow and localized fault bounded slice tectonics (LFBST): insights from petrological, structural, geochronological and geospeedometric studies in the Sikkim Himalaya, NE India. Lithos 282–283:464–482

Cubas N, Avouac JP, Souloumiac P, Leroy Y (2013a) Megathrust friction determined from mechanical analysis of the forearc in the Maule earthquake area. Earth Planet Sci Lett 381:92–103

Cubas N, Avouac JP, Leroy YM, Pons A (2013b) Low friction along the high slip patch of the 2011 Mw 9.0 Tohoku-Oki earthquake required from the wedge structure and extensional splay faults. Geophys Res Lett 40:4231–4237

Das JP, Bhattacharyya K, Mookerjee M, Ghosh P (2016) Kinematic analyses of orogen-parallel L-tectonites from Pelling-Munsiari thrust of Sikkim Himalayan fold thrust belt: insights from multiple, incremental strain markers. J Struct Geol 90:61–75

Dasgupta S, Pande P, Ganguly D, Iqbal Z, Sanyal K, Venkatraman NV, Dasgupta S, Sural B, Harendranath L, Mazumdar K, Sanyal S, Roy K, Das LK, Misra PS, Gupta H (2000) Seismotectonic Atlas of India and its environs. Geological Survey of India, Calcutta, pp 14–15

Dasgupta S, Ganguly J, Neogi S (2004) Inverted metamorphic sequence in the Sikkim Himalayas: crystallization history, P–T gradient and implications. J Metamorph Geol 22:395–412

Dasgupta S, Mukhopadhyay B, Mukhopadhyay M, Nandy DR (2013) Role of transverse tectonics in the Himalayan collision: further evidences from two contemporary earthquakes. J Geol Soc India 81:241–247

De R, Kayal JR (2003) Seismotectonic model of the Sikkim Himalaya: constraint from microearthquake surveys. Bull Seismol Soc Am 93:1395–1400
De R, Kayal JR (2004) Seismic activity at the MCT in Sikkim Himalaya. Tectonophysics 386:242–248
Dotare T, Yamada Y, Adam J, Hori T, Sakaguchi H (2016) Initiation of a thrust fault revealed by analog experiments. Tectonophysics 684:148–156
Dumont T, Replumaz A, Rouméjon S, Briais A, Rigo A, Bouillin JP (2015) Microseismicity of the Béarn range: reactivation of inversion and collision structures at the northern edge of the Iberian plate. Tectonics 34:934–950
Dutta D, Biswas T, Mukherjee S (2019) Arc-parallel compression in NW Himalaya: evidence from structural and paleostress studies of brittle deformation from the clasts of upper Siwalik, Uttarakhand, India. J Earth Syst Sci. https://doi.org/10.1007/s12040-019-1138-1
Erslev EA (1993) Thrusts, back-thrusts and detachment of Rocky Mountain foreland arches. In: Schmidt CJ, Chase RB, Erslev EA (eds) Laramide basement deformation in the Rocky Mountain foreland of the western United States. Geol Soc Am Spec Pap 280:339–358
Gangopadhyay PK, Ray S (1978) Structures of Gorubathan area, Darjeeling district, West Bengal, with special reference to rock types and lead–zinc occurrence. Himal Geol 8:323–342
Ghose A (2006) Metallogenic characteristics in relation to tectonic framework of the Himalaya. Mem Geol Surv Ind 132:1–232
Ghosh P, Bhattacharyya K (2015) Examining microstructural and kinematic evolution of dominant thrust faults from hinterland of the Sikkim Himalayan FTB: insights into orogenic wedge deformation. In: Abstract Volume: 30th Himalaya–Karakoram–Tibet Workshop, Dehradun, India, 6–8 Oct 2015, pp 270–271
Ghosh S, Bose S, Mandal N, Dasgupta S (2016) Dynamic recrystallization mechanisms and their transition in the Daling Thrust (DT) zone, Darjeeling–Sikkim Himalaya. Tectonophysics 674:166–181
Ghosh S, Bose S, Mandal N, Das A (2018) Control on frontal thrust progression by the mechanically weak Gondwana horizon in the Darjeeling–Sikkim Himalaya. Tectonophysics 727:12–27
Godin L, Brown RL, Hanmer S, Parrish R (1999) Back-folds in the core of the Himalayan orogen: an alternative interpretation. Geology 27:151–154
Grujic D, Coutand I, Doon M, Kellett DA (2017) Northern provenance of the Gondwana Formation in the Lesser Himalayan Sequence: constraints from $^{40}Ar/^{39}Ar$ dating of detrital muscovite in Darjeeling–Sikkim Himalaya. Ital J Geosci 136:15–27
Hao S, Hua W, Long W, Hualing M, Yi L, Benjian Z (2016) Natural gas exploration prospect in the Upper Paleozoic strata, NW Sichuan Basin. Nat Gas Ind B 3:526–536
Harris NBW, Caddick M, Kosler J, Goswami S, Vance D, Tingle AG (2004) The pressure–temperature–time path of migmatites from the Sikkim Himalaya. J Metamorph Geol 22:249–264
Hazarika P, Kumar MR, Srijayanthi G, Raju PS, Rao NP, Srinagesh D (2010) Transverse tectonics in the Sikkim Himalaya: evidence from seismicity and focal-mechanism data. Bull Seismol Soc Am 100:1816–1822
He D, Webb AAG, Larson KP, Martin AJ, Schmitt AK (2015) Extrusion vs. duplexing models of Himalayan mountain building 3: duplexing dominates from the oligocene to present. Int Geol Rev 57:1–27
Hodgson CJ (1989) The structure of shear-related, vein-type, gold deposits: a review. Ore Geol Rev 4:231–273
Hu X, Garzanti E, Wang J, Huang W, An W, Webb A (2016) The timing of India-Asia collision onset—facts, theories, controversies. Earth Sci Rev 160:264–299
Hubbard MS (1996) The role of ductile shear in metamorphic inversion, a Himalayan example. J Geol 104:493–499
Iaccarino S, Montomoli C, Carosi R, Massonne H-J, Visonà D (2016) Geology and tectono-metamorphic evolution of the Himalayan metamorphic core: insights from the Mugu Karnali transect, Western Nepal (Central Himalaya). J Metamorph Geol 35:301–325
Jain AK, Manickavasagam RM (1993) Inverted metamorphism in the intracontinental ductile shear zone during Himalayan collision tectonics. Geology 21:407–410
Jayangondaperumal R, Kumahara Y, Thakur VC, Kumar A, Srivastava P, Dubey S, Dubey AK (2017) Great earthquake surface ruptures along backthrust of the Janauri anticline, NW Himalaya. J Asian Earth Sci 133:89–101
Koehn D, Passchier CW (2000) Shear sense indicators in striped bedding-veins. J Struct Geol 22:1141–1151
Kroehler ME, Mann P, Escalona A, Christeson GL (2011) Late Cretaceous-Miocene diachronous onset of back-thrusting along the South Caribbean deformed belt and its importance for understanding processes of arc collision and crustal growth. Tectonics 30:TC6003
Lahiri S (1973) Some observations on structure and metamorphism of the rocks of Kurseong-Tindharia region, Darjeeling district, West Bengal. Himalayan Geol 3:365–371
Landry KR, Coutand I, Whipp DM, Grujic D, Hourigan JK (2016) Late Neogene tectonically driven crustal exhumation of the Sikkim Himalaya: insights from inversion of multithermochronologic data. Tectonics 35:833–859
Li J, Mitra S (2017) Geometry and evolution of fold-thrust structures at the boundaries between frictional and ductile detachments. Mar Pet Geol 85:16–34
Li Z, Liu-Zeng J, Jia D, Sun C, Wang W, Yuan Z, Liu B (2016) Quaternary activity of the range front thrust system in the Longmen Shan piedmont, China, revealed by seismic imaging and growth strata. Tectonics 35:2807–2827
Little TA (2004) Transpressive ductile flow and oblique ramping of lower crust in a two-sided orogen: insight from quartz grain-shape fabrics near the Alpine fault, New Zealand. Tectonics 23:1–24
Luo Y, Ampeuro JL (2018) Stability of faults with heterogeneous friction properties and effective normal stress. Tectonophysics 733:257–272
Mahato S, Mukherjee S, Bose N (2019) Documentation of brittle structures (back shear and arc-parallel shear) from Sategal and Dhanaulti regions of the Garhwal Lesser Himalaya (Uttarakhand, India). In: Mukherjee S (ed) Tectonics and structural geology: Indian context. Springer International Publishing, Cham, pp 411–423. ISBN: 978-3-319-99340-9
Mandl G (2005) Rock joints. Springer, Berlin, p 1-221. ISBN 978-3-540-26457-6
Martin A (2017a) A review of Himalayan stratigraphy, magmatism, and structure. Gondwana Res 49:42–80
Martin A (2017b) A review of definitions of the Himalayan Main Central Thrust. Int J Earth Sci 106:2131–2135
Matin A, Mazumdar S (2009) Deformation mechanisms in the frontal Lesser Himalayan Duplex in Sikkim Himalaya, India. J Earth Sys Sci 118:379–390
Meissner R (1989) Rupture, creep, lamellae and crocodiles: happenings in the continental crust. Terra Nova 1:17–28
Mitra G, Bhattacharyya K, Mukul M (2010) The lesser Himalayan duplex in Sikkim: implications for variations in Himalayan shortening. J Geol Soc Ind 75:289–301
Mohan A, Windley BF, Searle MP (1989) Geothermobarometry and development of inverted metamorphism in the Darjeeling–Sikkim region of the eastern Himalayan. J Metamorph Geol 7:95–110

Molinaro M, Guezou JC, Leturmy P, Eshraghi SA, de Lamotte DF (2004) The origin of changes in structural style across the Bandar Abbas syntaxis, SE Zagros (Iran). Mar Pet Geol 21:735–752

Montomoli C, Ruggieri G, Carosi R, Dini A, Genovesi M (2005) Fluid source and pressure–temperature conditions of high-salinity fluids in syn-tectonic veins from the Northeastern Apuan Alps (Northern Apennines, Italy). Phys Chem Earth 30:1005–1019

Montomoli C, Carosi R, Iaccarino S (2015) Tectonothermal discontinuities in the Greater Himalayan Sequence: a local or a regional feature? In: Mukherjee S, Carosi R, van der Beek PA, Mukherjee BK, Robinson D. 2015. Tectonics of the Himalaya. Geol Soc London Spec Publ 402:25–41

Mottram CM, Warren CJ, Regis D, Roberts NM, Harris NB, Argles TW, Parrish RR (2014a) Developing an inverted Barrovian sequence; insights from monazite petrochronology. Earth Planet Sci Lett 403:418–431

Mottram CM, Argles TW, Harris NBW, Parrish RR, Horstwood MSA, Warren CJ, Gupta S (2014b) Tectonic interleaving along the Main Central Thrust, Sikkim Himalaya. J Geol Soc 171:255–268

Mottram CM, Warren CJ, Halton AM, Kelley SP, Harris NBW (2015) Argon behaviour in an inverted Barrovian sequence, Sikkim Himalaya: the consequences of temperature and timescale on $^{40}Ar/^{39}Ar$ mica geochronology. Lithos 238:37–51

Mugnier JL, Delcaillau B, Huyghe P, Leturmy P (1998) The break-back-thrust splay of the Main Dun Thrust (Himalayas of western Nepal): evidence of an intermediate displacement scale between earthquake slip and finite geometry of thrust systems. J Struct Geol 20:857–864

Mukherjee S (2013a) Channel flow extrusion model to constrain dynamic viscosity and Prandtl number of the Higher Himalayan Shear Zone. Int J Earth Sci 102:1811–1835

Mukherjee S (2013b) Higher Himalaya in the Bhagirathi section (NW Himalaya, India): its structures, backthrusts and extrusion mechanism by both channel flow and critical taper mechanisms. Int J Earth Sci 102:1851–1870

Mukherjee S (2014) Atlas of shear zone structures in meso-scale. Springer Geology, Cham, p 1-124. ISBN 978-3-319-0088-6

Mukherjee S (2015) Atlas of structural geology. Elsevier, Amsterdam. ISBN: 978-0-12-420152-1

Mukherjee S, Koyi HA (2010a) Higher Himalayan Shear Zone, Zanskar section—microstructural studies and extrusion mechanism by a combination of simple shear and channel flow. Int J Earth Sci 99:1083–1110

Mukherjee S, Koyi HA (2010b) Higher Himalayan Shear Zone, Sutlej section—structural geology and extrusion mechanism by various combinations of simple shear, pure shear and channel flow in shifting modes. Int J Earth Sci 99:1267–1303

Mukherjee S, Punekar J, Mahadani T, Mukherjee R (2015) A review on intrafolial folds and their morphologies from the detachments of the western Indian Higher Himalaya. In: Mukherjee S, Mulchrone KF (eds) Ductile shear zones: from micro- to macro-scales. Wiley Blackwell, pp 182–205

Mukhopadhyay DK, Mishra P (2005) A balanced cross section across the Himalayan frontal fold-thrust belt, Subathu area, Himachal Pradesh, India: thrust sequence, structural evolution and shortening. J Asian Earth Sci 25:735–746

Mukhopadhyay DK, Chakraborty S, Trepmann C, Rubatto D, Anczkiewicz R, Gaidies F, Dasgupta S, Chowdhury P (2017) The nature and evolution of the Main Central Thrust: structural and geochronological constraints from the Sikkim Himalaya, NE India. Lithos 282:447–463

Mukul M (2000) The geometry and kinematics of the Main Boundary Thrust and related neotectonics in the Darjiling Himalayan fold-and-thrust belt, West Bengal, India. J Struct Geol 22:1261–1283

Mukul M (2010) First-order kinematics of wedge-scale active Himalayan deformation: insights from Darjiling–Sikkim–Tibet (DaSiT) wedge. J Asian Earth Sci 39:645–657

Mukul M, Jade S, Ansari K, Matin A (2014) Seismotectonic implications of strike–slip earthquakes in the Darjiling–Sikkim Himalaya. Curr Sci 106:198–210

Najman Y, Jenks D, Godin L, Boudagher-Fadel M, Millar I, Garzanti E, Bracciali L (2017) The Tethyan Himalayan detrital record shows that India–Asia terminal collision occurred by 54 Ma in the Western Himalaya. Earth Planet Sci Lett 459:301–310

Namson JS, Davis TL (1988) Seismically active fold and thrust belt in the San Joaquin Valley, central California. Geol Soc Am Bull 100:257–273

Nath SK, Vyas M, Pal I, Sengupta P (2005) A seismic hazard scenario in the Sikkim Himalaya from seismotectonics, spectral amplification, source parameterization, and spectral attenuation laws using strong motion seismometry. J Geophys Res 110:B01301

Neogi S, Dasgupta S, Fukuoka M (1998) High P–T polymetamorphism, dehydration melting, and generation of migmatites and granites in the Higher Himalayan Crystalline Complex, Sikkim, India. J Pet 39:61–99

Oxburgh ER (1972) Flake tectonics and continental collision. Nature 239:202–204

Parui C, Bhattacharyya K (2018) Duplex and along-strike structural variation: a case study from Sikkim Himalayan fold thrust belt. J Struct Geol 113:62–75

Passchier CW, Trouw RAJ (2005) Microtectonics, 2nd edn. Springer, Berlin, p 1-366. ISBN-10 3-540-64003-7

Patel RC, Singh P, Lal N (2015) Thrusting and back-thrusting as post-emplacement kinematics of the Almora klippe: insights from low-temperature thermochronology. Tectonophysics 653:41–51

Patro PK, Harinarayana T (2009) Deep geoelectric structure of the Sikkim Himalayas (NE India) using magnetotelluric studies. Phys Earth Planet Int 173:171–176

Paul DK, McNaughton NJ, Chattopadhyay S, Ray KK (1996) Geochronology and geochemistry of the Lingtse Gneiss, Darjeeling-Sikkim Himalaya: revisited. J Geol Soc India 48:497–506

Platt JP, Lister GS, Cunningham P, Weston P, Peel F, Baudin T, Dondey H (1989) Thrusting and backthrusting in the Brianqonnais domain of the western Alps. In: Coward MP, Dietrich D, Park RG (eds) Alpine tectonics. Geol Soc Spec Publ 45:135–152

Pradhan R, Prajapati SK, Chopra S, Kumar A, Bansal BK, Reddy CD (2013) Causative source of Mw 6.9 Sikkim-Nepal border earthquake of September 2011: GPS baseline observations and strain analysis. J Asian Earth Sci 70–71:179–192

Prakash D, Tewari S (2013) Field and textural relationship in pelitic schists and gneisses from the area around Mangpu, Darjeeling district, West Bengal. J Geol Soc Ind 81:451–454

Price RA (1986) The southeastern Canadian Cordillera: thrust faulting, tectonic wedging, and delamination of the lithosphere. J Struct Geol 8:239–254

Pyne TK, Gangopadhyay PK (1976) Structural characteristics of the Buxa Group in the Buxa Duar region, Jalpaiguri district, West Bengal. Himal Geol 6:247–258

Robinson DM, Pearson ON (2013) Was Himalayan normal faulting triggered by initiation of the Ramgarh–Munsiari thrust and development of the Lesser Himalayan duplex? In: Mukherjee S, Mukherjee, B, Thiede R (eds) Geosciences of the Himalaya–Karakoram–Tibet Orogen. Int J Earth Sci 102:1773–1790

Rodgers DA, Rizer WD (1981) Deformation and secondary faulting near the leading edge of a thrust fault. In: McClay KR, Price NJ (eds) Thrust and nappe tectonics. Geol Soc London Spec Publ 9:65–77

Rubatto D, Chakraborty S, Dasgupta S (2013) Timescales of crustal melting in the Higher Himalayan Crystallines (Sikkim, Eastern

Himalaya) inferred from trace element-constrained monazite and zircon chronology. Contrib Miner Petrol 165:349–372
Saha D (2013) Lesser Himalayan sequences in eastern Himalaya and their deformation: Implications for Paleoproterozoic tectonic activity along the northern margin of India: Geosci Front 4:289–304
Samimi S, Gholami E (2017) Geometric and kinematic analysis of structural elements along north front of Bagharan Kuh Mountain, NE Iran. Geotectonics 51:192–208
Sammis CG, Steacy SJ (1995) Fractal fragmentation in crustal shear zones. In: Barton CC, La Pointe PR (eds) Fractals in the earth sciences. Springer, New York, pp 179–204
Schultz RA (2000) Localization of bedding plane slip and backthrust faults above blind thrust faults: keys to wrinkle ridge structure. J Geophys Res Planets 105:12035–12052
Searle MP, Szulc AG (2005) Channel flow and ductile extrusion of the high Himalayan slab-the Kangchenjunga–Darjeeling profile, Sikkim Himalaya. J Asian Earth Sci 25:173–185
Shah SBA, Abdullah WH (2017) Structural interpretation and hydrocarbon potential of Balkassar oil field, eastern Potwar, Pakistan, using seismic 2D data and petrophysical analysis. J Geol Soc Ind 90:323–328
Singh P, Patel RC (2017) Post-emplacement kinematics and exhumation history of the Almora klippe of the Kumaun–Garhwal Himalaya, NW India: revealed by fission track thermochronology. Int J Earth Sci 106:2189–2202
Sinha Roy S (1973) Kinematic significance of conjugate folds in the Daling Metamorphites from Kalimpong Hills, Sikkim Himalaya. Himal Geol 3:176–184
Srivastava P, Mitra G (1994) Thrust geometries and deep structure of the outer and lesser Himalaya, Kumaon and Garhwal (India): implications for evolution of the Himalayan fold-and-thrust belt. Tectonics 13:89–109
Sun J, Shen ZK, Li T, Chen J (2016) Thrust faulting and 3D ground deformation of the 3 July 2015 Mw 6.4 Pishan, China earthquake from Sentinel-1A radar interferometry. Tectonophysics 683:77–85
Thakur VC, Pandey AK, Suresh N (2007) Late Quaternary-Holocene evolution of dun structure and the Himalayan Frontal fault zone of the Garhwal sub-Himalaya, NW India. J Asian Earth Sci 29:305–319
Tiwari VM, Rao MV, Mishra DC, Singh B (2006) Crustal structure across Sikkim, NE Himalaya from new gravity and magnetic data. Earth Planet Sci Lett 247:61–69
Trepmann CA, Stöckhert B (2009) Microfabric of folded quartz veins in metagreywackes: dislocation creep and subgrain rotation at high stress. J Metamorph Geol 27:555–570
Vassallo R, Mugnier JL, Vignon V, Malik MA, Jayangondaperumal R, Srivastava P, Carcaillet J (2015) Distribution of the late-Quaternary deformation in Northwestern Himalaya. Earth Planet Sci Lett 411:241–252
Webb AAG, He D (2012) The South Tibetan Detachment is a backthrust: new evidence from studies along the length of the Himalayan orogeny. In: Abstract Volume of the 27th Himalaya–Karakoram–Tibet workshop. J Nepal Geol Soc 45:1
Webb AAG, Yin A, Harrison TM, Célérier J, Gehrels GE, Manning CE, Grove M (2011) Cenozoic tectonic history of the Himachal Himalaya (northwestern India) and its constraints on the formation mechanism of the Himalayan orogeny. Geosphere 7:1013–1061
Webb AAG, Guo H, Clift PD, Husson L, Müller T, Costantino D, Yin A, Xu Z, Cao H, Wang Q (2017) The Himalaya in 3D: slab dynamics controlled mountain building and monsoon intensification. Lithosphere 9:637–651
Xu S, Fukuyama E, Ben-Zion Y, Ampuero JP (2015) Dynamic rupture activation of backthrust fault branching. Tectonophysics 644:161–183
Yin A (2006) Cenozoic tectonic evolution of the Himalayan orogen as constrained by along-strike variation of structural geometry, exhumation history, and foreland sedimentation. Earth Sci Rev 76:1–131
Zelilidis A, Papatheodorou G, Maravelis AG, Christodoulou D, Tserolas P, Fakiris E, Ferentinos G (2016) Interplay of thrust, backthrust, strike-slip and salt tectonics in a fold and thrust belt system: an example from Zakynthos Island, Greece. Int J Earth Sci 105:2111–2132
Zhang G, Hetland EA, Shan X, Vallée M, Liu Y, Zhang Y, Qu C (2016) Triggered slip on a back reverse fault in the Mw 6. 8 2013 Lushan, China earthquake revealed by joint inversion of local strong motion accelerograms and geodetic measurements. Tectonophysics 672:24–33
Zhao J, Yuan X, Liu H, Kumar P, Pei S, Kind R, Wang W (2010) The boundary between the Indian and Asian tectonic plates below Tibet. Proc Natl Acad Sci 107:11229–11233
Zuppetta A, Mazzoli S (1997) Deformation history of a synorogenic sedimentary wedge, northern Cilento area, southern Apennines thrust and fold belt, Italy. Bull Geol Soc Am 109:698–708